Universidade do Minho
Escola de Ciências

Vanessa Tatiana Pinho

Development of liposomal vectors for effective delivery of pleiotropic recombinant leukemia inhibitory factor (LIF) cytokine

janeiro de 2020

Vanessa Tatiana Pinho **Development of liposomal vectors for effective delivery of pleiotropic recombinant leukemia inhibitory factor (LIF) cytokine**

UMinho | 2020

Universidade do Minho
Escola de Ciências

Vanessa Tatiana Pinho

Development of liposomal vectors for effective delivery of pleiotropic recombinant leukemia inhibitory factor (LIF) cytokine

Dissertação do Mestrado
Mestrado Bioquímica Aplicada Especialização em Biomedicina

Trabalho efetuado sob a orientação de
Professora Doutora Andreia Ferreira Castro Gomes
Professora Maria Elisabete da Cunha Dias Real Oliveira

janeiro de 2020

Acknowledgments

Agradecimentos, uma secção não menos importante que o resto desta tese porque o trabalho faz-se em equipa.

Queria agradecer à Professora Andreia pelo tempo disponibilizado, atenção e ajuda. Ela ensina-nos não só como trabalhar com profissionalismo, mas também como sermos melhores no nosso dia-a-dia.

Também tenho de agradecer imenso à Professora Elisabete pela partilha da sua sabedoria sobre fundamentos físicos e o tempo disponibilizado para me introduzir os nanossistemas.

Duas pessoas fundamentais neste percurso o Doutor Raúl e o Doutor André, a quem não posso deixar de agradecer a ajuda e a atenção.

O Ivo e ao Mário, os primeiros a iniciar esta caminhada comigo, tenho de agradecer a ajuda para começar este caminho.

A Anabela, uma pessoa fundamental no grupo, que não poderia deixar de agradecer, pelo tempo disponibilizado para me ouvir, para me ajudar e para me obrigar a almoçar.

Queria agradecer em especial à Catarina e à Sofia pela boa companhia, pela partilha de ideias, pelas brincadeiras sem sentido e pelo carinho que certamente será relembrado. Não poderia de deixar de agradecer à Luana e aos peixes ("infelizmente alguns não estão mais presentes") o tempo e o carinho disponibilizados (espero que a dieta seja cumprida). Apesar de pouco tempo com a Sofia M. quero agradecer-lhe os risos que ajudaram nestes momentos de mais "stress" e será certamente uma pessoa que não será esquecida. Ao Pedro, tenho de agradecer a sua boa amizade que foi importante em momentos menos bons. Tenho de agradecer à Rita e Sara pela sua boa disposição e pela ajuda.

Em último, mas das pessoas mais importantes, queria agradecer aos meus pais, por aguentarem a minha pessoa, por me comprarem café e não chá e pela ajuda a ver pormenores que nem eles sabem o que são.

Statement of integrity

I hereby declare I conducted this academic work with integrity. I confirm that I have not used plagiarism or any form of undue use of information or falsification of results along the process leading to its elaboration.

I further declare that I have fully acknowledged the Code of Ethical Conduct of the University of Minho.

Resumo

LIF é uma citocina pleiotrópica que é capaz de desencadear efeitos terapêuticos para o tratamento de leucemia, regeneração muscular, doenças neurológicas e infertilidade, entre outros. Esta citocina é rapidamente eliminada *in vivo* e é capaz de desencadear efeitos benéficos e desfavoráveis em diferentes tipos de células. Deste modo, o principal objetivo deste trabalho é encapsular a LIF em lipossomas DODAB:MO (1:2) e validar este sistema em duas linhas celulares, C2C12 e M1.

O sistema lipossomal DODAB:MO foi previamente estudado pelo grupo e foi demonstrada a sua capacidade para transportar proteínas, mas não citocinas. O sistema DODAB:MO (1:2) é caracterizado pela capacidade de formar agregados invertidos não-lamelares no interior do lipossoma, permitindo assim a solubilização de uma grande quantidade de proteína. Para validar estes nanotransportadores nos modelos celulares, era importante o uso de baixas concentrações de lípido de forma a minimizar a citotoxicidade. Por conseguinte, foi usado DODAB:MO (1:2) numa concentração de 0.4mM e 10 μg/mL de LIF, sendo possível a produção de nanopartículas estáveis em dois pH diferentes (5 e 7.4). Estes transportadores eram também, positivamente carregados (60-70mV), tinham um tamanho pequeno (~170nm) e uma alta eficiência de encapsulação (>80%). Analisando as características físicas do transportador, este tem o potencial para aplicado como transportador de moléculas terapêuticas.

Os modelos celulares usados foram mioblastos (linha celular C2C12) e mieloblastos de leucemia (linha celular M1) de ratinho. Na linha celular C2C12, pequenas concentrações de LIF são responsáveis pela proliferação e atraso da diferenciação celular. Culturas inicialmente plaqueadas a uma densidade de $1x10^4$ cells/mL, foram responsivas a proliferação com as concentrações 0.001 e 0.1 ng/mL de LIF, avaliada por ensaios SRB e "Hoechst". As células C2C12 são capazes de diferenciação em miotubos com 2% de HS sem mascarar os efeitos de proliferação, sendo uma opção para ensaios de proliferação com LIF. Relativamente à linha celular M1, baixas concentrações de LIF promovem a proliferação, mas não a diferenciação. A proliferação foi averiguada com ensaios "Hoechst" e azul tripano e mostraram que células a uma densidade inicial de $3x10^4$ cells /mL obtiveram uma baixa taxa de proliferação desencadeadas pelas concentrações 0.01 and 1 ng/mL de LIF, e uma maior percentagem de viabilidade.

Em ensaios futuros, é necessário (i) testar outros ensaios *in vitro* para validar as concentrações de LIF, (ii) validar o sistema DODAB:MO encapsulando LIF nos modelos celulares e (iii) produzir um novo transportador com LIF ancorada à superfície.

Palavras-chave: DODAB:MO lipossomas, citocina LIF, mieloblastos, mioblastos

Abstract

Leukemia inhibitory factor (LIF) is a pleiotropic cytokine that can trigger therapeutic effects in leukemia disease, muscle tissue regeneration, neurological diseases and infertility problems. This cytokine has high rates of clearance *in vivo* and the capability to trigger beneficial and detrimental functions in different cell types. The main goal of this work was to encapsulate LIF in dimethyldioctadecylammonium bromide (DODAB): monoolein (MO) (1:2) liposomes and validate the system in two cell models, C2C12 and M1 cell lines.

The DODAB:MO liposomal system was previously well studied by our research group for protein delivery but not cytokines in particular. The DODAB:MO (1:2) system is characterized by the ability to form inverted non-lamellar phases inside the liposome core, solubilizing high amounts of protein. In order to validate these nanocarriers in cell models, lower lipid concentrations were used to minimize cytotoxicity. Using 0.4mM of DODAB:MO (1:2) and 10 μg/mL LIF, it was possible to produce a stable nanoparticle at two pH conditions (5 and 7.4). This nanocarrier was positively charged (60-70mV), small (~170 nm mean size) with high encapsulation efficiency (>80%). Based on the physical characteristics of this nanocarrier, it may have potential to be applied as a therapeutic option.

The cell models used were murine myoblasts (C2C12 cell line) and myeloid leukemia cells (M1 cells). In C2C12 cells, lower LIF concentrations are responsible for cell proliferation and differentiation delay. In cultures with an initial seeding cell density of $1x10^4$ cells/mL, 0.001 and 0.1 ng/mL LIF led to higher proliferation rates, assessed with SRB and Hoechst assays. C2C12 cells are capable to differentiate forming myotubes, and 2% of horse serum (HS) instead of 5% HS in culture medium demonstrated to boost differentiation in presence of LIF, without masking proliferation. Low LIF concentrations can stimulate M1 proliferation but not their differentiation into macrophages. Proliferation was studied with the Hoechst assay and viability with the trypan blue assay. The results show that at $3x10^4$ cells /mL, lower proliferation rates were observed with 0.01 and 1 ng/mL LIF concentrations, but also higher viability.

In future experiments, it is necessary to (i) test other *in vitro* assays to validate LIF concentrations, (ii) validate the DODAB:MO carrier encapsulating LIF in the cell models and (iii) produce another carrier with LIF adsorbed at the liposome surface.

Key Words: DODAB:MO liposomes, LIF cytokine, myoblasts, myeloblasts

Scientific Outputs

Scientific Publications

1. Vanessa Pinho, Mário Fernandes, André da Costa, Raúl Machado, Andreia C. Gomes (2019) "Leukemia inhibitory factor: Recent advances and implications in biotechnology", *Cytokine & Growth Factor Reviews,* DOI 10.1016/j.cytogfr.2019.11.005

Poster communication

1. Poster communication entitle "DODAB:MO versus Novel liposomes for protein delivery: comparing toxicity and encapsulation efficiency" – Vanessa Pinho, Mário Fernandes, Ana C.N. Oliveira, Ivo Lopes, Claúdia Botelho, José A.Teixeira, M. Elisabete C.D.Real Oliveira, Andreia C.Gomes - in the 8th Iberian Meeting on Colloids and Interfaces (RICI8) – 17 to 19 of July 2019, Aveiro, Portugal.
2. Poster communication entitle "DODAB:MO versus Novel liposomes for protein delivery: comparing toxicity and encapsulation efficiency" - Vanessa Pinho, Mário Fernandes, Ana C.N. Oliveira, Ivo Lopes, Claúdia Botelho, José A.Teixeira, M. Elisabete C.D.Real Oliveira, Andreia C.Gomes – Jornadas CF-UM-UP 2019 – 13 of December of 2019, Braga, Portugal.

Table of Contents

List of abbreviations and acronyms

Acute lymphoblastic leukemia (ALL)

Acute myeloid leukemia (AML)

Bovine serum albumin (BSA

By Dulbecco's Modified Eagle Medium (DMEM)

Chronic lymphocytic leukemia (CLL)

Chronic myelogenous leukemia (CML)

Critical packing parameter (P)

Dimethyldioctadecylammonium bromide (DODAB)

Dimethylsulfoxide (DMSO)

Dioctadecyl- dimethylammonium chloride (DODAC)

Escherichia coli (E.coli)

Fetal Bovine Serum (FBS)

Glycoprotein 130 (gp130)

Granulocyte colony stimulating factor (G-CSF)

Granulocyte colony stimulating factor receptor (G-CSF R)

Granulocyte- macrophage colony stimulating factor (GM-CSF)

Growth factor receptor-bound protein (GRB2)

Horse Serum (HS)

Hydrogen ions (H^+ ions)

Hydroxide (OH^-) ions

Insulin-like growth factor-1 (IGF-1)

Interleukin 6 (IL-6)

Janus kinases – signal transducer and activator of transcription factor (JAK-STAT)

Leukemia inhibitory factor (LIF)

LIF receptor (LIFR)

Lipid/protein (L/P)

Macrophage colony stimulating factor receptors (M-CSF R)

Mitogen-activated protein kinase (MAPK)

Monoolein (MO)

Murine LIF receptor (mLIFR)

Myeloid leukemia cell line (M1)

Myoblast determination protein (myod)

Myoblasts cell line (C2C12)

Myocyte enhancer factor 2 (MEF2)

Nanostructured lipid carriers (NLC)

Penicillin-Streptomycin (P-S)

Phosphoinositide 3-kinase (P3IK).

Poly-(ethylene glycol) (PEG)

Protein inhibitor of the activated STAT (PIAS)

Protein kinase inhibitor (H7)

Self-double drug delivery systems emulsifying (SDEDDS O/O/W)

Self-nanoemulsifying drug delivery systems (SDEDDS W/O/W)

Solid lipid nanoparticles (SNL)

Sulforhodamine B (SRB)

Suppressor of the cytokine signaling (SOC)

Tyrosine kinase inhibitor (tyrphostin)

Figure Index

Table Index

Equation Index

1. Introduction

1.1. Leukemia inhibitory factor

Interleukin 6 (IL-6) family of cytokines is composed by several cytokines as: IL-6, interleukin-31, interleukin-27, oncostatin M, cardiotrophin-1, cardiotrophin-like cytokine factor 1, ciliary neurotrophic factor and LIF [1,2]. Cytokine is a soluble protein capable of transmit intercellular signals in the same local (adjacent cells; in the same cell that produced it), or in distinct organs [3]. Despite being pleiotropic, these proteins have redundant activity. This activity can be caused by evidences of gp130 sharing receptors and action on the same cell [3]. All members of this family can promote diversified functions in inflammation, immunity or even cancer [1,2].

Leukemia inhibitory factor (LIF) is a pleiotropic cytokine that prompt distinct functions depending on the tissues or organs where it is present [1,2]. The intracellular effects triggered by this protein (LIF) can be, among others, proliferation and differentiation, very easy to assess. Because of that, this protein can be used to validate *in vitro* models.

LIF has 202 aminoacids [4] and four alpha-helixes' stabilized by three disulfide bridges crucial for activity preservation , and the N-terminal region important to receptor binding **(Fig.1)** [2,5,6].

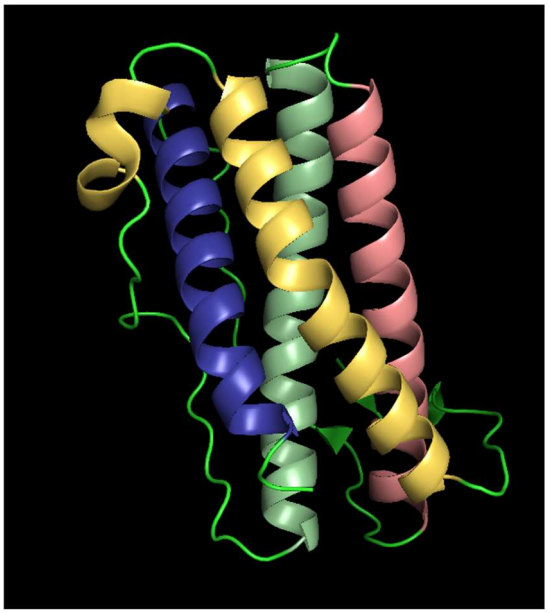

Figure 1 Alpha-helix's structure of *Mus Musculus* LIF. Helix A – Yellow; Helix B – Pale green; Helix C – Dark Pink; Helix D – Blue. *Draw in PyMOL*. [7].

A common feature between IL-6 family elements is the presence of the cytokine receptor unit, glycoprotein 130 (gp130) in their receptors structure. Regarding LIF, it has a heterodimer receptor that comprised not only the gp130 unit but also, the signal transducing receptor β- subunit. Protein-receptor binding at the cell surface promotes activation of intracellular pathways for instance: janus kinases – signal transducer and activator of transcription factor (JAK-STAT), mitogen-activated protein kinase (MAPK) and phosphoinositide 3-kinase (P3IK). The overall functions triggered by the latter pathways are survival, apoptosis, differentiation and proliferation **(Fig.2)** [2] .

Nevertheless, LIF is a pleiotropic cytokine and as a result, the main mechanisms activated after receptor-protein interaction can be distinct depending on the cell type. [2,8,9].

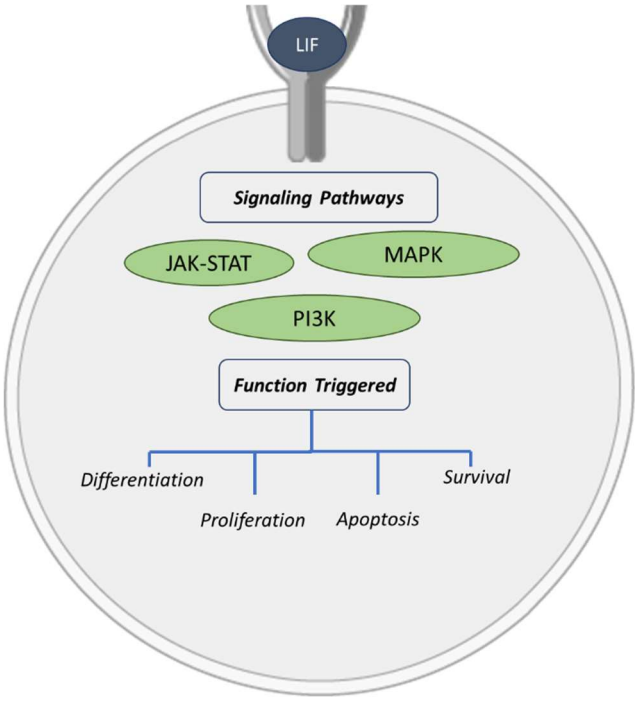

Figure 2 The LIF cytokine binds to the corresponding receptor and can activate three different pathways: JAK-STAT, RAS-RAF-ERK and PI3K. Depending of the cell type, the function triggered can be different: differentiation, proliferation, survival or apoptosis [2].

LIF affinity to the receptor can be dependent on LIF origin. LIF protein may or may not bind to receptor of another species depending on its origin. This event is well studied with murine and human receptor upon human LIF binding [10]. A study of LIF receptor (LIFR) α-chain disclose the Ig-like domain predominant role for the phenomenon of mouse specific binding to murine LIF receptor (mLIFR) and human cross reactivity with mLIFR and human LIFR [10]. Despite murine [11], and human [12], being the most used LIF sources, it has been isolated and characterized from different animals, such as buffalo

[13], cat [14] and brushtail possum [15]. The homologies regarding human, mouse and other sources are between 70 and 90%, showing a highly conserved structure among species [11–15].

For experimental use, the most commonly used LIF is produced by organisms such as *Escherichia coli (E.coli)* [16,17], plants [18,19] and viruses [20,21]. *E.coli* is the less expensive model and the one with the highest rate of protein production [12,22]. The least chosen hosts are plants or mammalian cells because of the lower protein production and the need of a more exhaustive process of purification. Nevertheless, new techniques are being optimized and a plant source, rice, has been used recently to produce LIF [19]. Regarding different hosts for heterologous production, a question about glycosylation and its importance in LIF function was assessed. Although, it became elucidated that there are no relevant effects on LIF function whenever post-translational modification is present or absent [23–25]. This could be related to the fact that glycosylation is a post-translational modification, that allows the protein portection *in vivo*, preventing it from being degraded [26].

Considering articles toward the past five years with LIF as a potential therapeutic target, the research areas with most publications are related to infertility and endometrium receptivity. Also there are a low number of articles related to muscle regeneration and cancer, emphasizing potential themes to be explored [27].

Because of the above reasons and because of the rate of proliferation and easy manipulation, for this work, myoblasts cell line (C2C12) and myeloid leukemia cell line (M1) were chosen to explore the LIF effects.

1.2. Effects triggered by LIF in muscle cells

Skeletal muscle is the tissue in the body with more activity and is composed majority by water and proteins. The skeletal muscle is composed by muscle fibers, associated to a conjunctive tissue, blood vessels and nerves. [28,29].

In general muscle injuries follow three stages: the acute inflammatory and degenerative phase (1 to 3 days) characterized by activation and infiltration of immune cells; the repair phase (3 to 4 weeks) responsible for macrophages activation and scar tissue formation; and the remodeling phase (3 to 6 months) responsible for myofibers regeneration. Focusing on the second phase the activated macrophages [30] have two essential functions: firstly, they remove the necrotic myofibers by phagocytosis; and secondly, generate, together with fibroblasts, chemotactic signals [31]. Despite that, the extracellular matrix also contains growth factors that become active when the tissue is damaged. Some of this growth factors responsible for activate satellite cells are: fibroblast growth factor, insulin-like

growth factor-1 (IGF-1), insulin-like growth factor-2, transforming growth factor-β, tumor necrosis factor-α, and IL-6 [32]. The regeneration phase or third phase, consists in the regeneration of the disrupted myofibers [31], process based in the differentiation of muscle stem cells and maturation of regenerated fibers **(Fig.6)** [30].

Immediate treatments for injuries in skeletal muscles are: (a) RICE (rest, ice, compression and elevation); (b) Medication, mostly anti-inflammatory drugs (NSAIDs) to diminish the inflammatory reaction [33]; (c) physiotherapy; (d) surgical treatment, normally just for grade III injuries [34].

.

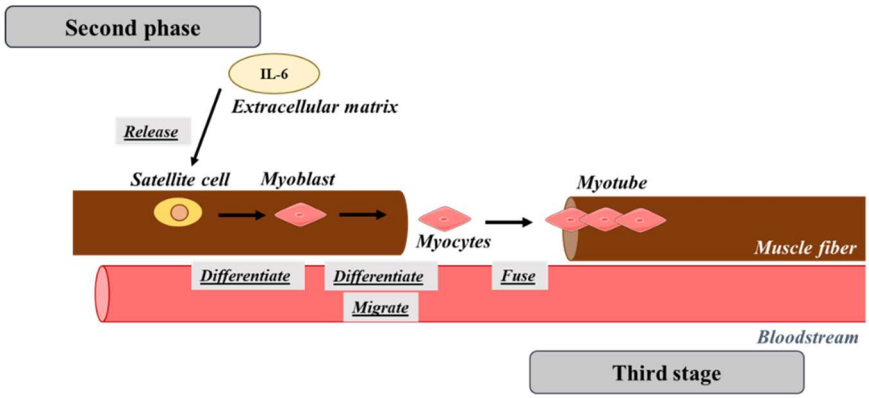

Figure 3 Satellite cells differentiate into myoblasts that migrate to the injury site and differentiate in myocytes. At this point, a process of fusion begins in order to produce myotubes and regenerate the injury muscle [30].

New strategies have been proposed, for instance, the use of growth factors and gene therapy. Growth factors and cytokines are suggested because of the capability to be potent mitogenic activators, important in regeneration phases for the formation of new myotubes [32]. It has been demonstrated that IL-6 is responsible for migration, proliferation and differentiation of myoblasts, playing a significant role in muscle stem cells, and for myotubes formation [30]. IL-6 family is composed by several cytokines *(described in section 1.1 Leukemia Inhibitory factor)* such as LIF, a known proliferation and differentiation promotor of muscle cells [23,35].

In order to study the response of LIF in muscle cells, for this work, C2C12 cell line was chosen as an *in vitro* model. C2C12 is a immortalized myoblast line of *Mus musculus* from mouse [36]. This line was chosen due to the visible effects upon differentiation (formation of myotubes very distinguishable) [37], higher rates of proliferation, and the potential to elucidate of LIF effects in muscle cells .

Studies with LIF establish the role of proliferation and differentiation in muscle cells [2,35,38]. A study in 1991, by Austin and Burgess, determine that LIF, from all other cytokines, for example IL-6 and IGF-1, showed the higher potential for growth stimulation in myoblasts from mice of the C57-BL-10 strain. Also, this researchers got defined the maximal concentration of LIF for maximum proliferative response as being approximately 0,012 ng/mL [35]. Although, cells exposed to LIF concentrations between 0,1-0,3 ng/mL, undergo proliferative effects that could last up to 13 days [38]. Recently, more studies showed the importance of LIF concentration to start proliferation or differentiation in C2C12 cells. Demonstrating that LIF promote myoblasts proliferation and delay differentiation, if present in low concentrations. A concentration of 0,1 ng/mL decreases the number of myotubes in 50% and if stimulated with 20 ug/mL of LIF, cells almost cannot differentiate [23].

LIF stimulate proliferation and delay differentiation activating signaling pathways when bind to the LIF receptor. The pathways evolved in LIF-induced proliferation are the JAK-STAT signaling [39] and the Ras–Raf–MEK-ERK pathway (Fig.4) [39]. During proliferation **(Fig.4A)**, the mechanism JAK-STAT initiates when LIF binds to the receptor and activate by phosphorylation the Janus Kinase 1 (JAK1). Then, JAK1´s phosphorylate tyrosine residues in the intracellular domain of the receptor allowing STAT1proteins [39] and growth factor receptor-bound protein (GRB2) to attach it [40]. STAT1 becomes phosphorylated and available to form a STAT dimer. The dimer STAT1 bind to myocyte enhancer factor 2 (MEF2) protein [39,41], and then bind to specific regions of DNA, decreasing the transcription of differentiation proteins (for example: myoblast determination protein (MyoD)) [39]. MEF2 protein is a final product of RAS-MEK-ERK pathway, as a result of GRB2 phosphorylation at the receptor intracellular domain [40].

Proliferation and differentiation mechanisms rely on mutually inhibiting signals to perform the respective functions. Differentiation **(Fig.4B)** is triggered by low concentrations of LIF and is regulated at intracellular level by negative regulators such as: suppressor of the cytokine signaling (SOC) and protein inhibitor of the activated STAT (PIAS). The three main negative regulators in myoblasts are SOC1, SOC3 and PIAS1 and inhibit JAK1, gp130 domain and STAT1, respectively [42]. STAT3 dimer play an important role in differentiation complexing MyoD protein. This complex attaches to specific regions of DNA in nucleus, responsible for the production of differentiation factors [39,43].

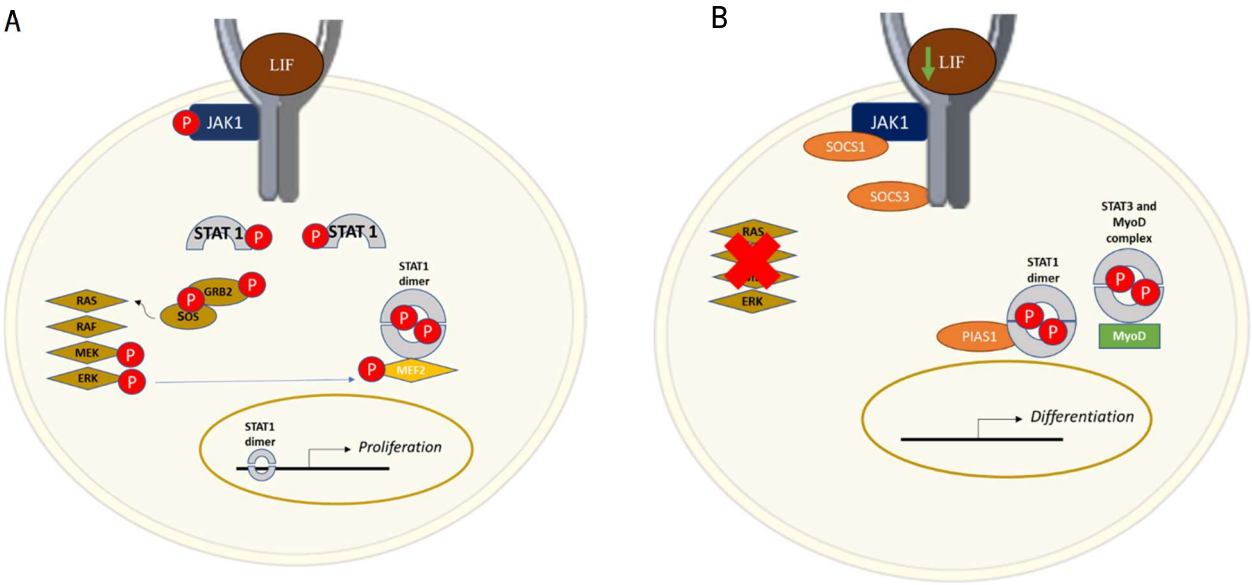

Figure 4 A- During proliferation, LIF binds to the receptor phosphorylating JAK1 [39]. Therefore, the tyrosine residues from the intracellular domain of gp130 are also phosphorylated, activating STAT1[39] and GRB2 [40]. STAT1 dimer associate with MEF2 protein [39,41], resulting from the RAS-MEK-ERK pathway [40], enter the nucleus of myoblasts and bind to regions of DNA in order to decrease the transcription of differentiation proteins [39]. **B-** The presence of low concentrations of LIF became possible the process of myoblast differentiation. The differentiation process is controlled by negative regulators as: SOC1, SOC3 and PIAS1. SOC1 binds JAK1, SOC3 target gp130, and PIAS1 have as a target STAT1 [42]. MyoD binds to activated STAT3 dimer, complex that bind in the nucleus sites responsible to produce differentiation proteins [39,43].

In summary, balancing LIF concentrations is important to promote myoblasts proliferation and differentiation. This is a cell model where the functions triggered by LIF are well described in the literature and can be assessed *in vitro.* Also, having a nanocarrier transporting LIF and release it in a controlled way is important to validate this system, comparing to LIF added directly without a transporting system.

1.3. Effects of LIF in myeloid leukemia cells

The potential therapeutic effect of LIF in cancer has been poorly explored in the past five years [27]. Leukemia, an aggressive cancer, is described as production of abnormal white cells (myeloblast or lymphoblast). The classification of leukemia disease types is based on the type of blood cells that are affected, and the speed of disease development. Despite all types of leukemia can occur in adults and children, this disease is more prone to develop in individuals older than 50 [44] and younger than 15 [44,45].

Leukemia disease is divided into four categories: acute lymphoblastic leukemia (ALL), acute myeloid leukemia (AML), chronic myelogenous leukemia (CML) and chronic lymphocytic leukemia (CLL)

[44]. The standard treatments for almost all types of leukemia are chemotherapy, radiotherapy and targeted therapy [46–49]. Focusing on LIF, not all types of leukemia cells are influenced by this cytokine. In ALL disease, LIF expression is stimulated by healthy stromal cells and indirectly allow the survival of leukemic cells [50], despite that, no other studies were found. Respecting CLL disease, LIF levels were undetectable [51], rejecting a possible effect of LIF in this cells. Another type of leukemia disease without LIF effects, in this case not explored, is CML, that is considered a heterologous genetic disease and a search for a therapy is based on understanding the interactions of mutated genes with BCR-ABL1 oncogene [52]. In the other hand, a very promising approach with growth factors, have been used as therapeutic molecules to treat AML since 1987 [53]. Those molecules are granulocyte- macrophage colony stimulating factor (GM-CSF) and granulocyte colony stimulating factor (G-CSF) and they are responsible for survival, proliferation and maturation of myeloid precursors [53,54].

Leukemia inhibitory factor is also an important factor that promote differentiation of myeloid leukemia cells *in vitro* [55], phenomenon that did not occur *in vivo*. Regardless of the *in vitro* results, blast progenitors were isolated from AML patients and examined by blast colony assay, indicating that fresh AML blasts did not differentiate when exposed to LIF. In that study, the results emphasizing the importance of combine other cytokines as GM-CSF, interleukin-3 and IL-6 with LIF to potentiate the proliferation effect [56]. A quick research about currently clinical trials using LIF to treat AML show no results [57,58].

In 1969, Ichikawa, established the myeloid leukemia cells, M1, isolated from SL strain mice, *in vitro.* The cells were not capable of differentiation into macrophages and neutrophil granulocyte without stimulation [59]. M1 cell line are myeloblasts from leukemia and this cell line is from *Mus musculus*, mouse. This cell line has a high proliferative rate and they grow in suspension [59].

For differentiation and proliferation stimulation, LIF activates LIF receptor, and therefore the related pathways **(Fig.5).** One of the many activated signaling cascades is the JAK-STAT pathway. In this extension, STAT3 dimers are formed and bind to genes promoter regions in order to promote differentiation and growth arrest [60]. These regions grant transcription of myeloid differentiation primary response 88 (MyoD88) genes [60,61] and suppression of c-myb transcription factor [60]. The latter is an early factor that is responsible for leukemic phenotype maintenance that is absent when M1 cells differentiate. Another transcription factor responsible for leukemogenicity is c-myc transcription factor, and in order to promote M1 differentiation is necessary the suppression of this factor [62]. Despite STAT3 could promote differentiation, when in higher quantities can trigger apoptosis [60].

Another triggered pathway to promote differentiation is SLC (T-cell acute lymphocytic leukemia 1) pathway [63]. SLC activation is characterized by an increase of: (i) lysozymes [63] important to acute leukemia diagnosis indicating the presence of monoblastic differentiation [64], and (ii) Mac1-α [63], an adhesion molecule present in monocytic subtypes of acute leukemia, allowing adhesion and migration of hematopoietic cells [65]. An independent pathway (SLC-independent) activated is responsible for the increase of macrophage colony stimulating factor receptors (M-CSF R) [66,67] and granulocyte colony stimulating factor receptor (G-CSF R) [67]. Thus, a phenomenon of differentiation occurs in M1 cells.[66,67].

On the other hand, kinase inhibitors such as nonspecific protein kinase inhibitor (H7) and tyrosine kinase inhibitor (tyrphostin) were identified as targets for inhibition of differentiation on M1 inhibiting MyoD genes [61].

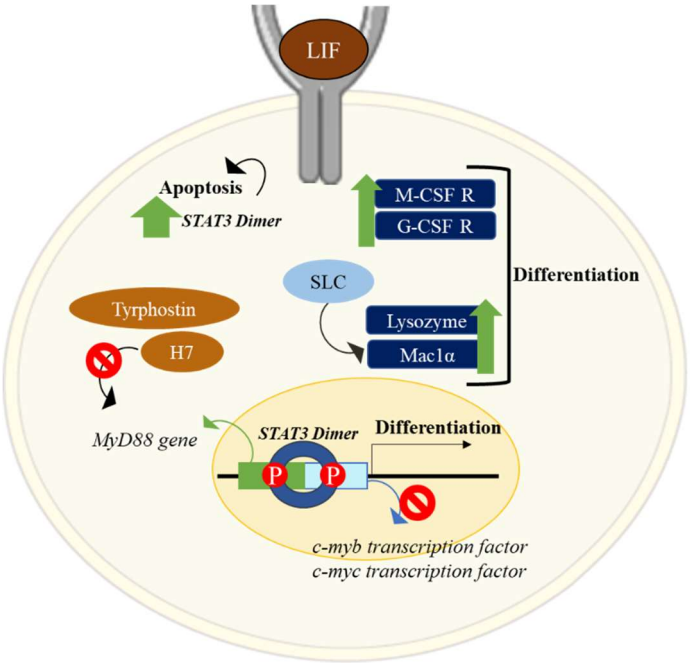

Figure 5 LIF binds to the receptor and three pathways are activated: JAK/STAT [60,61], SLC and SLC independent [63]. STAT3 dimer produced from the activation of JAK/STAT pathway binds to DNA regions responsible for c-myb and c-myc transcription factor inhibition and MyoD88 gene production [60–62] Although, Tyrphostin and H7 are responsible for differentiation inhibition through MyoD88 gene blockage [61]. Also, apoptosis can be triggered when STAT3 is at higher quantities. SLC pathway leads to an increase of lysozyme and Mac1-α, and an independent pathway allows the increase of M-CSF R and G-CSF R. Together, these two pathways can promote differentiation [63].

As reported by Youngblood and colleagues [19], different concentrations of LIF stimulate M1 cells to proliferate, differentiate or survive. The group used as LIF concentrations: 0,004; 0,04; 0,4; 4 and 40 ng/mL. They demonstrate that 50% of M1 cells are prevented to grow in the presence of 0,21 ng/mL of

LIF. In summary, when M1 cells are incubated with LIF at higher concentrations, differentiation is stimulated, and proliferation is inhibited.

This literature results demonstrate that M1 is a simple cell model to assess LIF activity and because low concentrations are used, the importance of controlled release and protein stability are important. Also, the nanocarriers functionalization, avoid unintended results in other cells. Due to that facts, nanocarriers can be validate in this model as being more advantageous than LIF without a carrier.

1.4. Nanotechnology

The term nanotechnology has been used since mid-1980s, first described by Richard Feynman in his classic talk "There´s Plenty of Room at the Bottom" in 1961. The Feynman vision was building of nanomachines and other products by manipulating material atom by atom [68,69].

In 2000, the definition of nanotechnology was again re-elaborated and described as the ability to work at molecular level, atom by atom, in order to create large structures with a new molecular organization [68–70]. Because of this new perspective of nano scale, Smalley in 2000-2001, wrote about the fear that with nanotechnology manipulation, new life forms could appear, and self-replicate [71].

Nevertheless, curiosity about nanotechnology became stronger than the fear of the public, and more studies about nanotechnology applications appeared, based mainly in examples in Nature and categorized as nanoforms. Some examples of this biological nanoforms, are our muscles, ion channels and ribosomes [72]. Nowadays, nanotechnology has been applied in medicine, for diagnosis purposes and delivery of pharmacological or adjuvant substances to specific targets.

Nanocarriers can be produced by different materials and therefore divided into two main categories: inorganic nanoparticles, constituted by polymers, gold, silver, carbon, among others; and organic nanoparticles such as liposomes. Despite various nanotechnology formulations created, this work focuses on application and production of liposomal formulation and their importance in biomedicine applications [73,74]. Lipid based nanocarriers can be categorize into micelles, a structure of a single lipid layers where the head groups of the surface active-agents or surfactants with double tail (ex:Dimethyldioctadecylammonium bromide (DODAB), sphingomyelin, phosphatidylcholine, among others) forming bilayers when exposed to the solvent; inverted micelles similar to micelles but where the head groups are directed to the core of the particle; nanoemulsions, constituted by a single bilayer of oils and surfactants with their heads groups directed to the solvent; solid lipid nanoparticles (SNL) establish by saturated monoacid triglycerides single layer with a solid core at room temperature; nanostructured

lipid carriers (NLC) with a less organized solid core compared to the latter; ethosomes with a bilayer of phospholipids and more prone to be produced to skin application because the presence of ethanol in the composition; liposomes composed by a bilayer of phospholipids; and self-nanoemulsifying (SDEDDS W/O/W) and self-double emulsifying (SDEDDS O/O/W) drug delivery systems composed by oil, surfactants and drugs, unstable structures that when in contact with an aqueous environment produce nanoemulsions [75] **(Fig. 6)**.

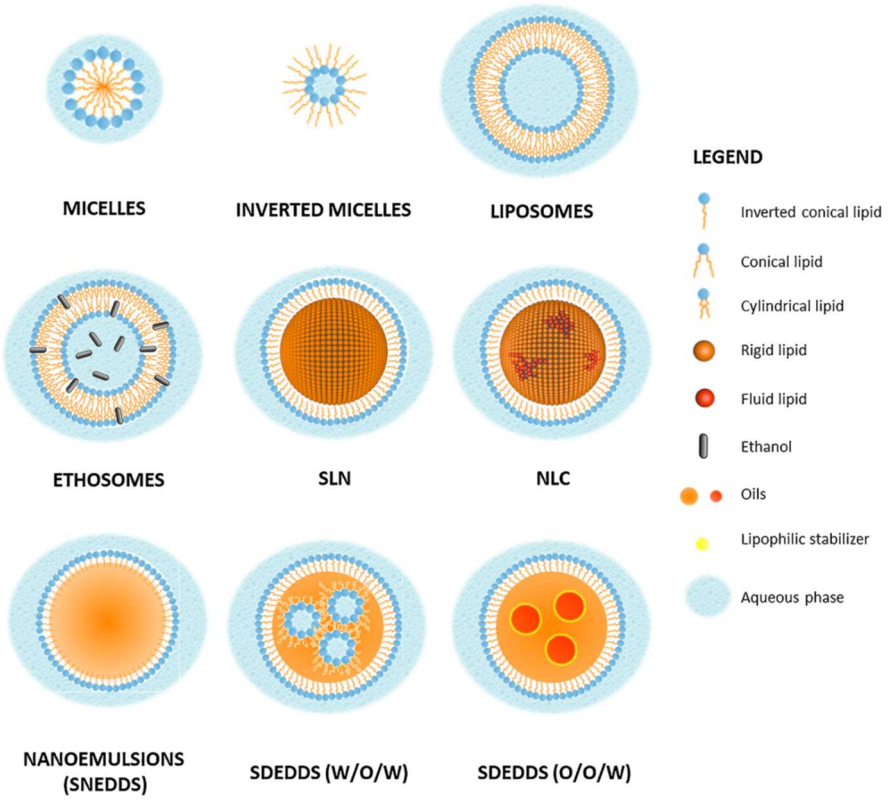

Figure 6 Types of lipid nanocarriers: micelles and inverted micelles composed by a single layer of surface active agents; liposomes constituted by a phospholipid bilayer; ethosomes that have ethanol in composition allowing more permeability; SLN and NLC composed by a solid core being the latter less organized and therefore more prone to encapsulate drugs; nanoemulsions that have in their composition oils and surfactants; SDEEDDS (W/O/W) and SDEDDS (O/O/W) constituted by oils, drugs and surfactants structure that when contact with an aqueous medium produce nanoemulsion [75].

Lipid nanocarriers have advantages and disadvantages that allow them to become a good option for *in vivo* applications such as diagnosis or therapy. The main advantages are the increasing life time of the substance encapsulated, targeting exclusively the intended local and capacity of controlled release of the therapeutic agent. On the other hand, the principal disadvantages are (i) the activation of the immune system, (ii) accumulation in other organs or tissues that are off the target, (iii) rapid elimination *in vivo*,

(iv) possibility to cause cell deformation *in vitro*, [76,77]. For better understanding the advantages and disadvantages it is necessary to study liposomal and lipids characteristics, for instance, structure, environmental behavior and type of lipids to be used [78].

1.4.1. Liposomes

Liposomes are small artificial spherical vesicles constituted by one or more phospholipids bilayers [78,79] with the polar groups of phospholipids oriented to the inner and outer aqueous phase [78] . They are spontaneously formed by hydrated phospholipids that are used for encapsulation of hydrophilic, hydrophobic and amphiphilic molecules such as DNA/RNA [74] and antigens [77].

The liposomal formation is created by a hydrophobic effect of lipid chains or tails causing desolvation of the hydration shell. The phenomenon begins with lipid tails contacting with a hydrophilic medium, triggering an immediate and spontaneous response to minimize contact, allowing the formation of organized structures [80]. The lipid membranes are not only an organized structure mimicked *in vitro* but also a nature structure resulting from lipid response to the medium. Other conformations can be created in laboratory based on the critical packing parameter (shape factor), temperature and medium composition. The shape factor allows the combination of lipid structural characteristics in an equation **(Eq. 1)** accomplishing a prediction of different structures formation, such as inverse (spherical, cubic, hexagonal), lamellar, cylindrical and spherical [81]. The parameters of the shape factor or critical packing parameter (P) related to lipids characteristics are headgroup area, molecular volume and length of hydrophobic tail **(Eq. 1)** [82].

$$Critical\ packing\ parameter = \frac{molecular\ volume}{head\ group\ area\ x\ maximum\ chain\ lenght}$$

Equation 1 Relation between molecular volume, head area and chain length of lipids in order to obtain a critical packing parameter.

Regarding lipid molecules with one single chain, if the head group increases the P decreases. Two types of structures can be produced: cylindrical monolayer if the head group is smaller, and spherical monolayer with a larger head group lipid **(Fig.7-A)**. However, phospholipids with two polyunsaturated chains can allow the production of other structures. With increasing size of the lipid head group and therefore a decrease of P, it is possible to produce spherical bilayer/ planar bilayer and also inverted non-bilayer structures **(Fig.7-B)**.

A

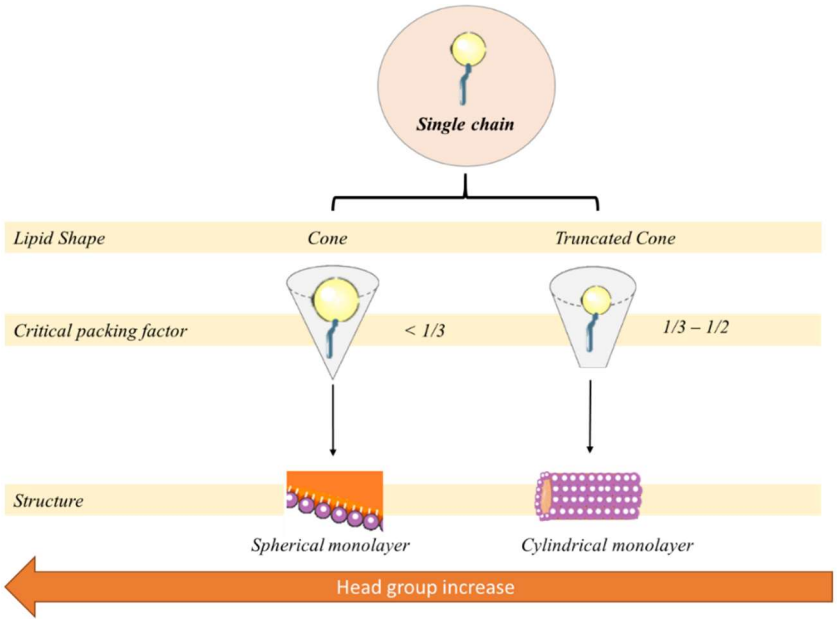

B

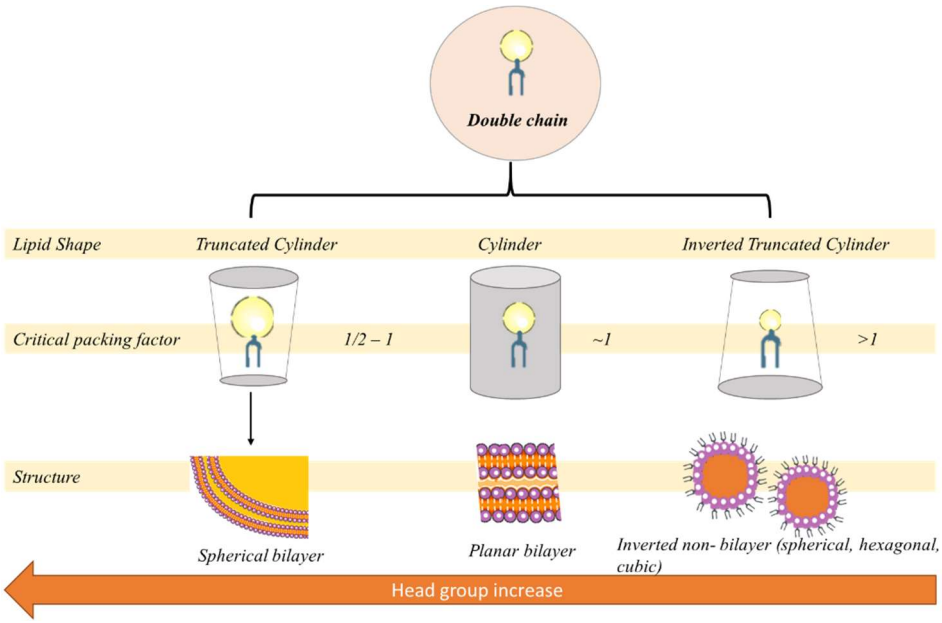

Figure 7 A- Lipids with one polyunsaturated chain can create two different structures depending on the head size. A bigger head group, results in a critical packing factor lower than 1/3 and allow the formation of spherical monolayers structures. On the other hand, a lipid with a small head group generate a cylindrical monolayer. **B-** For lipids with two polyunsaturated chains, considering an increasing size of the head group it is possible to form non-inverted, planar or spherical non-bilayers structures [82].

Depending on the environment a lipid molecule can also, behave differently [83,84]. Regarding the liposomal production it is necessary to take into account the particles aggregation and stabilization, highlighting study conclusions, such as, (i) smaller/neutral particles have a tendency to aggregate, (ii) bigger particles are more instable, (iii) particle functionalization allows more stabilization as a result of

the increased electrostatic repulsions (iv) and the increased salts in the medium allows more shell (superficial layer at the nanoparticle surface) hydration improving stabilization [85]. Functionalization is applied in order to produce liposomes targeting a specific tissue or organ and to mask the liposomes regarding the immune system [74,86,87]. For a future *in vitro/ in vivo* application, it is necessary to continue optimize the liposomal formulation in terms of Lipid/Protein concentration used, size and charge. Depending on size the nanoparticles can cross barriers and get to the target tissue or be lost in the biological system; and by masking the charge, nanoparticles can reach the target tissue without being eliminated by the immune system. Lipid/protein concentration is important to control the amount of protein delivered to the target cells.

In summary, for liposomal formulations lipid/protein molar fraction, size, charge, temperature and pH are important to attain the objective of delivery content without being detected by the immune system.

1.4.2. Cationic Liposomes as controlled delivery vectors

Our research group studied more specifically dioctadecyl- dimethylammonium bromide (DODAB) and dioctadecyl- dimethylammonium chloride (DODAC), cationic lipids, as conducive to create liposomes capable of encapsulating drugs or genetic material (siRNA/DNA) or proteins [88,89] [90][91][92].[87][93].

DODAB and DODAC differ in the hydrophilic head, this means that, DODAB possesses Br^- **(Fig.8)** as ion and DODAC possesses Cl^- as ion **(Fig.9)**. In solution Cl^- and Br^- ions behave differently. Chloride ion has a larger hydration shell, resulting in a lower screening of the positive charges of the cationic lipid head group in DODAC compared with DODAB. This allows a higher electrostatic repulsive forces between the heads and hydrophobic attraction between the tails, creating a cohesive spherical structure [88,94].

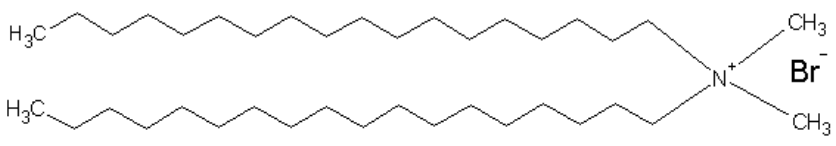

Figure 8 Line structure of DODAB. *Draw in ChemSketch.*

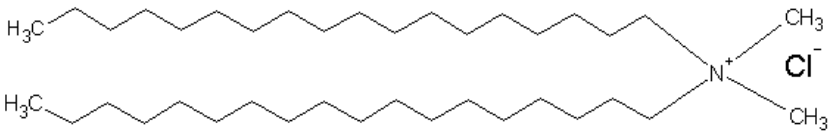

Figure 9 Line Structure of DODAC. *Draw in ChemSketch.*

Both cationic lipids produce lamellar structures similar to the bilayer from plasmatic membranes. The formulation based on DODAB give rises to a more compact structures, while DODAC produce less compact structures with higher destabilization and faster content release upon serum contact [94].

In order to increase the resistance and efficiency of delivery of DODAB and DODAC liposomes at physiological conditions, adjuvant lipids known as helper lipids are applied in the liposomal formulations [88,90–92].

The most used helper lipids are 1,2-dioleoyl-sn-glycero-3-phosphoethanolamine (DOPE), cholesterol and monoolein (MO) **(Fig.10)**. MO demonstrated to enable higher stability, controlled content release when the nanostructure reach the target, lower toxicity and efficient cell internalization [90].

The importance of MO in DODAX lipidic structures is revealed in differential scanning calorimetry studies by evaluating the bilayer DODAX.MO fluidity as MO content increase. This phenomenon was also dependent on the counter ion and DODAX:MO molar fraction used [88] [95]. Another MO advantage is their tendency to form inverted non-lamellar structures. MO present in higher concentrations, grants more encapsulation of hydrophilic or hydrophobic substances inside the formulation, and as a consequence, an increase of solubilization of a specific substance [87,88,92,93].

Figure 10 Line structure of Monoolein. *Draw in ChemSketch.*

The incorporation of MO in liposomal DODAB/C is more homogenous distributed in the DODAC than DODAB bilayers, producing in the latter, enrich areas in MO, with impact in liposomal cell internalization. DODAB:MO (2:1) has higher internalization efficiency than DODAB:MO (1:2) and DODAC:MO (2:1) and (1:2), because DODAB enable the sphere shape from liposomes to have more curvature and therefore increases cell surface adherence [88]. The MO tendency to form non-lamellar structures (inverted non-lamellar phases) [88,92], promotes an increase in fusogenicity. This event may be related with the ability of cationic lipid to neutralize anionic lipids present in the plasmatic membrane, merging the membranes, allowing the liposomal content release into the cytoplasmatic environment [88]. Depending on DODAB/C:MO molar fraction of lipids, two different structures may be produced: (i) (2:1) more tendency to create lamellar phases; (ii) (1:2) the coexistence of non-lamellar and lamellar phases. The denominated non-lamellar phases or inverted lamellar aggregates are composed by MO, and is present in the liposome core, increasing the hydrophilic phases [88,90,94].

Liposomes can be plain or functionalized with a specific ligand, for example a ligand that binds to a surface receptor in the target tissue or organ, triggering function before internalization. The internalization might occurs via receptors/ or endocytose after interacting with the plasmatic membrane, and it can have three destinations: (i) be recycled; (ii) become trapped in the endosome that mature to a lysosome, destroying the carrier; (iii) or it can escape the endosome and release the content in the cell interior [74] [86]. The cationic lipids DODAB/C present some toxicity in the cells. Nevertheless, DODAC promote higher toxicity to cells than DODAB, being this effect diminish with MO content increasing [89]. Liposomes can be functionalized, more commonly with poly-(ethylene glycol) (PEG), in order to allow higher stabilization and increase half-time life *in vivo* [74,86,96–98]. These characteristics allow the protection of the liposome from immune system detection, more specifically, mask the surface charge of liposomes from being detected and directed to immune processes as protein opsonization or phagocytic internalization.

Briefly, DODAB and DODAC are two potential lipids for the creation of vehicles responsible for protein or DNA/RNA delivery. For more flexible and compatibly structures, MO can be incorporated in the design. The liposomal formulation can be functionalized with PEG for protection from the immune system for future applications *in vivo*. For protein encapsulation, the DODAB:MO (1:2) formulation is the better option because of the inverted phases in the core, allowing more protein to be solubilize and the chosen lipid DODAB is less toxic when the vehicle is disintegrated inside the cell [87,93].

2. Objective

The main goal of this thesis was to develop an effective, stable and safe liposomal formulation to deliver a pleiotropic cytokine, LIF, and its validation using two animal cell models, C2C12 myoblasts and M1 myeloid leukemia cells.

Due to rapid elimination of LIF *in vivo* and its pH sensitivity, our purpose was to encapsulate LIF in a DODAB:MO (1:2) liposomal formulation that has the potential to form inverted non-lamellar phases in the liposome's core, allowing more protein to be solubilized. This nanocarrier was previously used to successfully transport proteins, but not cytokines. Because LIF is pleiotropic, it can be a potential therapeutic agent for neurological diseases, infertility and respiratory problems, among others. The validation in two different cell models will allow inferring about future potential applications of this carrier as therapy.

To achieve the main goal, specific aims must be completed:

- Preparation of DODAB:MO (1:2) with different lipid/protein ratios, using BSA a model protein;
- Preparation of DODAB:MO (1:2) adsorbing LIF at the surface at ideal cytokine concentrations;
- Identify release profile of the systems;
- Characterization of the produced nanosystems in terms of size and surface charge;
- Assessment of the encapsulation efficiency by different methods;
- Studying the stability of the nanosystems in physiological conditions, at pH 5 and 7.4, and in contact with blood serum;
- Citotoxicity assessment;
- Optimization of parameters to assess LIF-mediated responses in C2C12 and M1 cell lines using commercial LIF.

This multidisciplinary work developed in this thesis is a partnership between the Biology Department and Physic Department from Minho University within the FUN2CYT project (FUN2CYT - Harnessing the potential for biomedical applications of pleiotropic cytokines LIF and oncostatin M, funded by Programa Operacional Competitividade e Internacionalização, POCI-01-0145-FEDER-030568).

3. Methods and Materials

3.1. Liposomes production

3.1.1. Lipid film hydration and Extrusion

Liposomes DODAB:MO (1:2) were produced by lipid film hydration using different lipid concentrations (1 mM and 0.2 mM). Stock solutions of DODAB (TCI, D1975) 20mM and MO (Sigma, M7765) 20 mM were prepared separately and dissolved in 100% ethanol (Fisher Scientific, CAS-64-17-5). The lipid film is produced pipetting for a glass tube the respective quantities of DODAB and MO, in order to produce the different lipid concentrations in a final volume of 5mL **(Table 1)**:

Table 1 Quantities of DODAB and MO to produce liposomes with 1mM and 0.2mM of lipid concentration.

Liposomal formulation	DODAB (µl)	MO (µl)
1mM	83.8	166.7
0.2mM	16.7	33.3

Next, the lipid film was formed using a rotary evaporator (Bibby Scientific Limited) for ethanol evaporation in a water bath (VWR) at 50°C, for 10 min. In order to hydrate the film in the rotary evaporator, a protein solution was added, in a bath of 50°C for 15 min. The process of liposome production was first optimized using 5 and 10 µg/mL of bovine albumin serum (BSA) (Sigma, A7030). BSA was used to substitute LIF (GenScript, Z03077) cytokine for optimization of lipid concentration to achieve a higher percentage of encapsulation efficiency and better stability.

After that, plain liposomes and encapsulating BSA were vigorously vortexed for 20s and were placed again in a water bath for another 20s, three cycles were perfomed. The next step was extrusion (Northern Lipids Inc.), at 50°C, using pressure at 8 atm, and with a 200 nm (Whatman, WHA110606) filter. Liposomes were characterized in the Zetasizer equipment (Malvern Zetasizer Nano ZS instruments) in terms of size and surface charge.

For production of empty liposomes, encapsulating BSA (10 and 20 µg/mL) and encapsulating LIF (10 and 20 µg/ml), the 0.4mM lipid concentration was used in a final volume of 7mL **(Table 2)**:

Table 2 Quantities of DODAB and MO to produce liposomes with 0.4mM lipid concentration.

Liposomal formulation	DODAB (µl)	MO (µl)
0.4mM	46.7	93.3

The process of extrusion was performed using a 400 nm (Whatman, WHA110607), 200 nm (Whatman, WHA110606) and 100 nm (Whatman, WHA110605) filters.

3.1.2. Encapsulation efficiency assessment

BSA quantification was accomplished by separation of encapsulated and non-encapsulated parts of the liposomal solution with Amicon® tubes (Merck) with a 100 nm pore. After centrifugation at 14 000 rpm for 20 min, the non-encapsulated part was separated at the tube bottom and the encapsulated part remained in the upper compartment.

Bradford method was optimized for lower BSA concentrations, in the interval of 0.1 ng/mL until 10 ng/mL. This technique is related with the presence of Coomassie Blue G250 dye in Bradford reagent. The solution color resulted from dye binding to proteins is dependent on the medium pH: neutral conditions is green, acidic conditions is red and blue in basic conditions [99,100]. When is not bound to a protein, the dye, has a 450nm absorbance, but upon binding it shifts to 595 nm [99]. The optimized method implied pipetting 150 µL from the Amicon® tube bottom part (non-encapsulated) and 150 µL of the Bradford reagent (Bio-Rad) to a 96 well plate. Next, the plate was incubated for 30 min at 37°C and read at 595 nm in a microplate reader (Molecular Devices, SpectraMax devices 384). The results obtained were confirmed using BSA-FITC.

In the case of LIF, the stock solutions 0.4mM liposomes with 10 µg/mL were diluted to achieve a concentration of 0.2mM liposomes 5 µg/mL LIF. The process for separation of the encapsulated and non-encapsulated parts was the same as for BSA, as was for the process with Bradford reagent. ELISA assays are more sensitive, and antibody based, yet more expensive and less practical. In order to validate the Bradford method, an ELISA kit for mouse LIF (Abcam, ab238261) detection was used following manufacturer´s instructions.

3.1.3. Stability

Stock solutions of liposomes were prepared by lipid film hydration followed by extrusion **(Table 3)**:

Table 3 Representation of the stock liposomes solutions used in the stability assay.

Liposomal formulation	BSA (µg/mL)	LIF (µg/mL)
0.4mM	10	10
0.4mM	20	not reliable data

The assay for measure stability of empty, encapsulating LIF and BSA, initiated by diluting 50mM of HEPES with a pH at 5 or 7.4 and 25 % of Fetal Bovine Serum (FBS) (Merck - S0615) in the respective liposomal solution. These solutions were important, because it is necessary to predict the performance of this systems in different pH, for example acidic environment in endosomes, and in biological fluids. The percentage of 25% was chosen based on previous work, where higher percentages (80%) of serum allowed the formation of bigger protein aggregates and increased mean size of liposomes [101]. Then, the solution was incubated at 37°C, and the liposomes were characterized in terms of size and surface charge, at eight timepoints: 0h, 30 min, 1h, 2h, 3h, 4h, 5h and 6h.

3.2. *In vitro* assays

Proliferation, differentiation and viability assays were made using two different animal cell lines to evaluate LIF biological effects and identify dose-dependent responses.

3.2.1. Cell maintenance

3.2.1.1. C2C12 cell line

C2C12 are myoblasts isolated from mouse, *Mus musculus*. They are adherent cells and can rapidly differentiate into myotubes [36].

Cells were maintained with complete medium (or proliferation medium) composed by Dulbecco's Modified Eagle Medium (DMEM) (Sigma, D56-48), 10% FBS and 1% Penicillin-Streptomycin (P-S) (Sigma - A5955) antibiotic mix, in a humidified incubator (Sanyo Electric Co.) at 37°C, with 5% CO_2 atmosphere.

For subculturing, cells were washed with PBS and disaggregated by incubation with 0.25% trypsin (Biochrom - L2103-20) for approximately 3 min at 37°C. The next step was trypsin inactivation with complete medium and 1:3 dilution of cells into a new culture flask. With the purpose of safeguarding the cell lines, they were also cryopreserved in liquid nitrogen. For that, cryopreservation medium constituted by complete medium and 5% of dimethylsulfoxide (DMSO) was used (Fisher Scientific, 67-68-5).

3.2.1.2. M1 cell line

M1 cells are myeloblasts from mouse, *Mus musculus,* and were established from spontaneous myeloid leukemia of SL strain mice. They grow in suspension and can be induced to differentiate into macrophages [59].

Cells were subcultured in a 60mm petri dish with density of $1x10^5$ cells/mL. The growth medium is Roswell Park Memorial Institute (RPMI) – 1640 (Biowest - L0498), supplemented with 10% FBS, 1% Penicillin-Streptomycin antibiotic mix, 2.0 g/L of sodium bicarbonate (Sigma, S5761), 4.5 g/L of D-glucose (Sigma - G8644), 10 mM HEPES (Sigma - H4034-100g) and 1mM sodium pyruvate (Sigma - S8636).

3.2.2. Proliferation assays

3.2.2.1. Sulforhodamine B dye

The SRB method can be used to assess proliferation rate. SRB binds to proteins in an acidic environment and can be extracted under basic conditions. When linked to proteins, a pink color appears. The pink color is then extracted with a basic solution, and the absorbance of the resulting colored solution measured in the spectrophotometer at 540nm. The amount of signal can be a measure of cell mass, and extrapolated to rates of cell proliferation [102].

C2C12 cells were initially seeded at $2x10^5$ cells/mL [40] but during optimization it was necessary to plated at $1.25x10^5$, in 12-well plates. The cells were left to adhere for 24h and the medium was renewed every 24h with LIF in 0.001, 0.01 or 1 ng/mL concentration [23,35] until 72h.

Cells were washed with PBS1x and a fixation solution (1% of acetic acid in methanol) was added and incubated for 1h 30 min, at a temperature of -20°C. The solution was discarded, and the plate was left to dry. Afterward, 0,5% SRB (Sigma, S9012) in 1% of acetic acid was added and the plate was incubated at 37°C for 1h 30 min. After incubation, the content was discarded, and the well was washed with 1% of

acetic acid (3 cycles). Again, the plate was left to dry, followed by addition of 10 mM Tris solution. The plate was agitated until the probe was well solubilize. The quantity of 200 µL was then transferred to a 96 well plate and absorbance read at 540 nm.

3.2.2.2. Hoechst Probe

Hoechst probe is usually used to stain nucleus for fluorescence, therefore it provides a way to measure the rate of proliferation based on nuclei count. With this method, cells were lysed and then incubated with the probe. Consequently, the emerged signal is a direct relation of DNA amount or number of cells in the sample [103].

A cell lysate was prepared with a solution of 15 mM Tris pH=7.4 and underwent a process of freeze-thaw twice. Next, 50 µL of the lysate is mixed with 50 µL of Hoechst probe (Sigma, 63493) at 5 µg/mL concentration in a 96 well plate. The absorbance is read using a fluorimeter (Thermo Scientific, Fluoroskan Ascent FL) with wavelengths of 350 nm for excitation and 460 nm for emission.

For validation of the SRB results, C2C12 cells were seeded at $1x10^5$ cells/mL in 12 well plates and left to adhere 24h. Cells were incubated with medium containing LIF in a 0.01 ng/mL concentration that was renewed every 24h until 72h. At each time point (24h, 48h and 72h) the medium was removed, cells washed with PBS and 15 mM Tris pH=7.4 added to the well. The Tris solution was pipetted vigorously against the well, in order to destroy the cell membrane and release the DNA. After obtaining the lysate, the process is the same as described above.

Upon optimization, C2C12 cells were plated at a density of $1x10^4$ cells/mL, in 6-well plates and the protocol repeated. The concentrations 0.01, 0.1 and 1 ng/mL of LIF were used and cells were maintained until the fifth day without intermediate measurements.

Regarding M1 cell line, cells were transferred from a 60mm petri dish when they reached the confluency, and seeded at $7x10^4$ cells/mL [19] in 24-well plates. Cells were seeded with growth medium containing LIF, at the concentrations of 0.001, 0.01 and 0.1 ng/mL [19]. On the third day, was added 250 µL of fresh growth medium with LIF in the respective concentration. At day five, cells were removed from the well to an microtube and were centrifuged at 500g for 8 min. The supernatant was discarded, and the pellet was resuspended in 15mM Tris pH=7.4. For proliferation evaluation, the process described above was performed.

3.2.3. Differentiation assay

To assess differentiation, an eosin and hematoxylin staining was performed. Eosin, an acidic probe with attraction for basic character structures, will stain cell cytoskeleton with a pink color, and hematoxylin, a basic probe, will appear with a purple color because of the capacity of attraction for acidic structures [37].

Differentiation assay with eosin and hematoxylin was performed to evaluate myotube formation. C2C12 cells were seeded at $1x10^5$ cells/mL in 12-well plates and medium was renewed daily for 7 days. The medium for differentiation is constituted by DMEM, 10%FBS, 1% Penicillin-Streptomycin antibiotic mix, and 2% Horse Serum (HS) (ThermoFisher, 16050122) or 5%HS.

At day 7, cells were washed twice with PBS and the cells were fixated with 100% methanol (Sigma – 179337) at -20°C temperature, for 20 min. Afterwards, the fixation solution was removed and the well washed with PBS. The staining was performed with 500 µL of hematoxylin (Merck, 105174) for 10 min, followed by a wash, staining with 300 µL eosin (Merck, 109844), for 5 min, and a final washing step. The plate was then left to dry.

To estimate if the number of cells increased during the differentiation process, Hoechst measurement was used in the same way as described in *3.3.2*.

3.2.4. Viability assay

Trypan blue assay is based on cell membrane viability, as the dye can only enter cells with damaged membranes. Cells with compromised membranes will appear in blue and cells with viable membranes without coloration [104]. This assay was used to extrapolate the results for toxicity evaluation. With this experiment, viability can be calculated with a simple mathematic equation **(Eq. 2)**:

$$\frac{Number\ of\ viable\ cells}{Number\ of\ viable\ cells + Number\ of\ non-viable\ cells} x100 = \%\ of\ Viable\ cells\ in\ the\ sample$$

Equation 2 Equation for calculation of viable cells in a sample.

In order to evaluate LIF cytotoxicity in M1 cells, cells were plated with a $7x10^4$ cells/mL density in 24-well plates [19]. Incubation with LIF started as soon as the cells were plated, with medium including LIF at a

suitable concentration. At day 3, 250 µL of growth medium with LIF was added to the wells. On day 5, cells were removed from the well. Afterwards, 20 µL of cell suspension was added to a microtube together with 20 µL of 0.4% trypan blue (Thermofisher Scientific, 15250061). The suspension was added to a Neubauer chamber and the viable cells (white) and non-viable cells (blue) were counted.

3.2.5. Toxicity assay

Cytotoxic assays were made to validate DODAB:MO (1:2) concentrations to be used *in vitro*. The toxicity of empty DODAB:MO was evaluated with hemolysis, using fresh blood from pig collected from the local butcher. The chosen concentrations were based in previous original work from the group [105]: 5 , 10 , 25, 50, 80 µg/mL.

Blood was washed with 100 µl of 0.9% saline solution and 200 µL of blood. Then, the solution was centrifuged at 600 g, 4°C for 5 minutes. If blood supernatant transparency is achieved, the pellet is resuspended in the saline solution and 100 µL of this solution is added to a microtube together with 100 µL of liposome solution. Microtubes are incubated at 37°C for 30 min and the final samples centrifuged at 600 g for 5 min. The supernatant was transferred to a 96 well plate and the absorbance read at 541 nm.

3.3. Statistical analysis

Statistical analysis was performed in GraphPad Prism 6.0 Software. Differences were considered if P was lower than 0.05. Statistical significance is highlighted as follow: * $p \leq 0.05$, ** $p \leq 0.01$, ***$p \leq 0.001$, **** $p \leq 0.0001$.

4. Results and Discussion

4.1. Liposomes characterization and BSA quantification

4.1.1. Liposomes production and characterization

DODAB:MO (1:2) carriers were produced using two lipid concentrations: 1mM and 0.2mM and encapsulating 5 and 10 μg/mL of BSA as model protein. Liposomes were characterized before and after extrusion in terms of size and surface charge **(Fig.11)**.

A

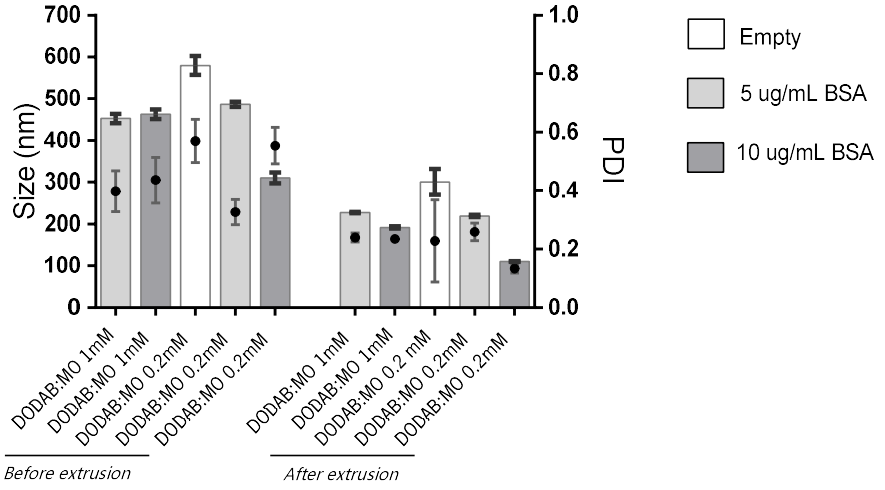

B

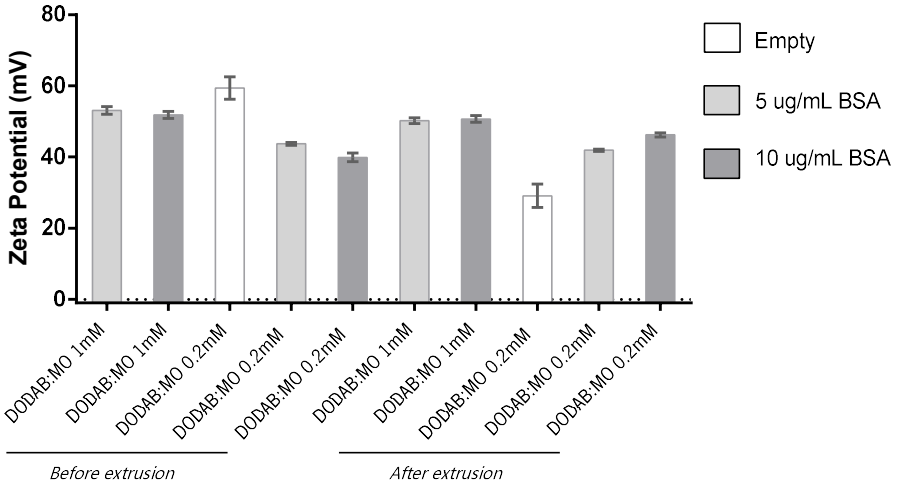

Figure 11 A- Size and **B-** Surface charge characterization for 1mM and 0.2mM DODAB:MO (1:2) empty and encapsulating 5 and 10 μg/mL of BSA.

After extrusion, all formulations decreased in size due to the 200 nm pore filter but remained positively charged regardless of being empty or encapsulating protein. This effect is because MO solubilizes the BSA in the liposomal core and DODAB, a cationic lipid, is at the surface being the main cause of the measured positive charge.

The physical characteristics of liposomes can be manipulated to achieve, for example, an ideal size and surface charge and also to find an optimal lipid/protein (L/P) ratio in order to achieve a good encapsulation efficiency.

4.1.2. BSA Encapsulation efficiency

In order to measure the encapsulation efficiency of the above formulations, the Bradford method was optimized as normally it is used for much higher protein concentrations.

Figure 12 represents a calibration curve obtained from the optimization of Bradford Method for a concentration in range of 0.1 µg/mL to 30 µg/mL of BSA.

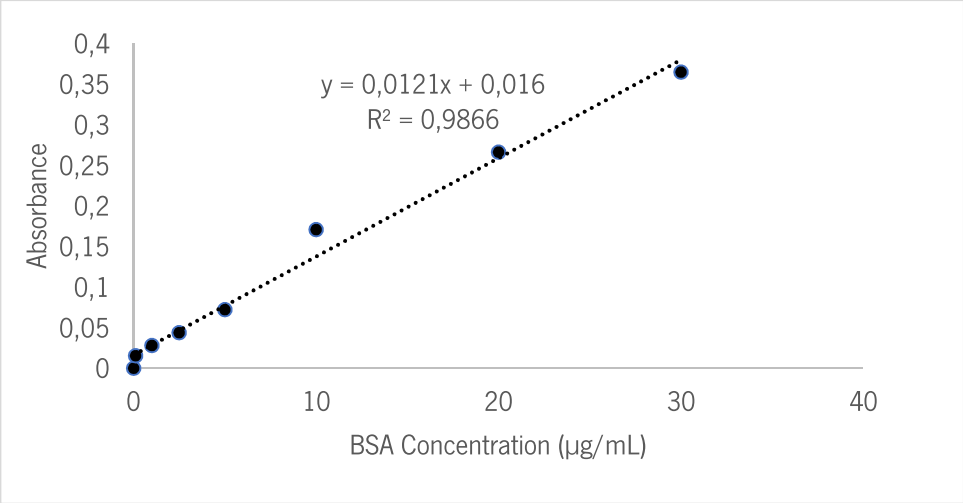

Figure 12 Calibration curve for BSA quantification by Bradford method for concentrations between 0.1 µg/mL to 30 µg/mL of BSA.

The lipid concentration 1mM and 0.2mM of DODAB:MO (1:2) mistures were used to encapsulate 5 and 10 µg/mL BSA solutions. Samples were then extruded and subject to centrifugation using amicons, to separate the encapsulated part (liposomes encapsulating BSA) from the non-encapsulated part. The results from the quantification of the non-encapsulated part by the Bradford method are on the next table and are a result of two independent assays (Table 4).

Table 4 Representation of the data of encapsulation efficiency for 0.2mM and 1mM DODAB:MO formulations encapsulating 5 and 10 μg/mL of BSA (n=2). Data analyzed by ANOVA (Tukey´s test): not statistically significant.

Liposomal formulation : $[BSA]_{Total}$	$[BSA]_{Encapsulated}$ (μg/mL)	Standard deviation	% Encapsulation Efficiency
0.2 mM:5 μg/mL BSA	4.118	2.773	82.369
1 mM:5 μg/mL BSA	2.906	5.942	58.127
0.2 mM10 μg/mL BSA	8.815	2.177	88.154
1 mM:10 μg/mL BSA	9.477	15.747	94.766

From the analysis of the previous results, the concentration of 0.2mM DODAB:MO have a higher encapsulation efficiency, with less discrepancy in standard deviation regardless of the protein concentration to be encapsulated. Despite that, the 1mM DODAB:MO:10 μg/mL of BSA has the best value for encapsulation efficiency, of almost 95%. Maintaining the same lipid concentration of 1mM but decreasing the BSA concentration for 5 μg/mL, the encapsulation efficiency is reduced to almost half of the value of the efficiency obtained for 1mM DODAB:MO:10 μg/mL BSA. The obtained results were statistically analyzed with ANOVA and are not statistically significant. This means that there are not relevant differences between the formulation, and the chosen condition can be independent of the encapsulation efficiency results.

In order to validate the results for encapsulation quantified with Bradford method, fluorescence from BSA-FITC was measured and the following calibration curve, between 0.1 and 10 μg/mL was obtained **(Fig.13)**.

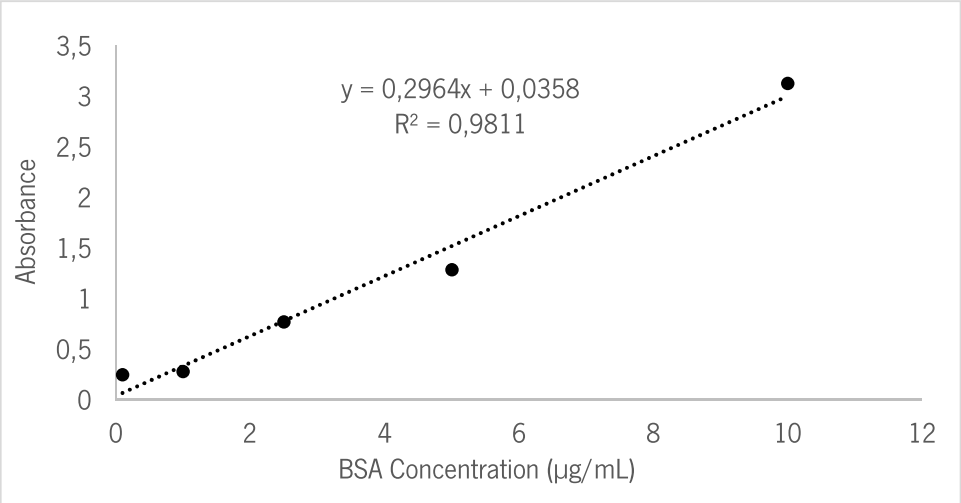

Figure 13 Graphical representation of the calibration curve for different BSA-FITC concentrations, between 0.1 µg/mL and 10 µg/mL.

The calibration curve of BSA-FITC was used to calculate the concentration of non-encapsulated BSA. This value was extrapolated to calculate the encapsulated BSA. This means that, for calculation it purposes, 5 ug/mL was considered the total concentration of BSA present in the two fractions (encapsulated and non-encapsulated) **(Table 5).**

Table 5 Representation of the results for encapsulation efficiency of 0.2mM and 1mM DODAB:MO formulations, encapsulating 5 and 10 µg/mL of BSA-FITC (n=1).

Liposomal formulation : $[BSA]_{Total}$	$[BSA]E_{ncapsulated}$ (µg/mL)	Standard deviation	% Encapsulation Efficiency
0.2 mM:5 µg/mL BSA	4.317	0.018	85.713
1 mM:5 µg/mL BSA	3.090	0.017	61.307
0.2 mM:10 µg/mL BSA	9.851	0.002	98.160
1 mM:10 µg/mL BSA	9.979	0.014	99.437

The quantification assay using fluorescence was performed in one independent assay and confirmed the results obtained with the Bradford method. This emphasizes the possibility of the latter being used as standard procedure to quantify protein at low concentrations. Analyzing the results from table 5, the best encapsulation efficiency is also obtained with 1mM DODAB:MO:10 µg/mL of BSA and higher percentages for 0.2mM encapsulating 5 and 10 µg/mL of BSA. Once again, the lower efficiency

was noted for 1mM DODAB:MO:5 µg/mL of BSA condition. This result could be related to an unbalance of the electrostatic and hydrophobic forces between the lipid molecules caused by the presence of BSA.

The percentage of encapsulation is different for each protein concentration even maintaining lipid concentration. There is a balance of forces that preserves the liposomal structure and responds uniquely for each protein and lipid concentration, making it impossible to compare the last two proportionally.

4.2. Liposomes characterization and LIF quantification

4.2.1. Liposomes production and characterization

Focusing on encapsulation efficiency results for BSA, two conditions were chosen to use with LIF, they were 0.2mM DODAB:MO encapsulating 5 and 10 µg/mL of protein. Both conditions have presented good results of protein encapsulation efficiency and despite the higher percentage of efficiency for 1mM DODAB:MO:10 µg/mL BSA, the future assays in cells, reinforce the use of less lipid. DODAB lipid is cytotoxic when becomes a single unit in the cell, separated from the liposomal structure [105], and this means choose the 0.2mM as lipid concentration.

To assess the encapsulation efficiency of LIF in DODAB:MO (1:2), 5, and 10 µg/mL of LIF it was chose in order to find the optimal L/P ratio to give a stable nanocarrier. The results from LIF cannot be compared to BSA results, despite the same values for lipid and protein concentrations, because lipid/protein ratios are not the same **(Table 6)**.

Table 6 Lipid/Protein ratios of 0.2mM liposomes encapsulating LIF and BSA.

[Lipid] (µM)	[LIF] (µg/mL)	[LIF] (µM)	[BSA] (µg/mL)	[BSA] (µM)	Lipid/Protein	Protein/Lipid
200	5	0.25	—	—	800	0.00125
200	10	0.5	—	—	400	0.0025
200	—	—	5	0.075	2666.7	0.000375
200	—	—	10	0.15	1333.3	0.000757

BSA protein has a higher molecular weight compared with LIF, so for the same mass concentration (µg/mL) it will present lower mass concentration compared to LIF. The number of

molecules of BSA to be encapsulated is lower than LIF. Due to lower molecular weight of LIF there will be more molecules to be encapsulated, for the same protein concentration.

In order to enable future stability assays, stock solutions were made of 0.4mM DODAB:MO encapsulating 10 and 20 μg/mL. of LIF. The lipid/protein ration is maintained and equal to 0.2mM 5 and 10 μg/mL of LIF **(Table 7)**.

Table 7 Ratio of Lipid/Protein of 0.4mM 10 and 20 μg/mL of LIF and 0.2mM 5 and 10 μg/mL of LIF.

[Lipid] (μM)	[LIF] (μg/mL)	[LIF] (μM)	Lipid/Protein
400	10	0.5	800
400	20	1	400
200	5	0.25	800
200	10	0.5	400

The 0.4mM DODAB:MO stock solutions were characterized in terms of size and surface charge **(Fig.14)**.

A

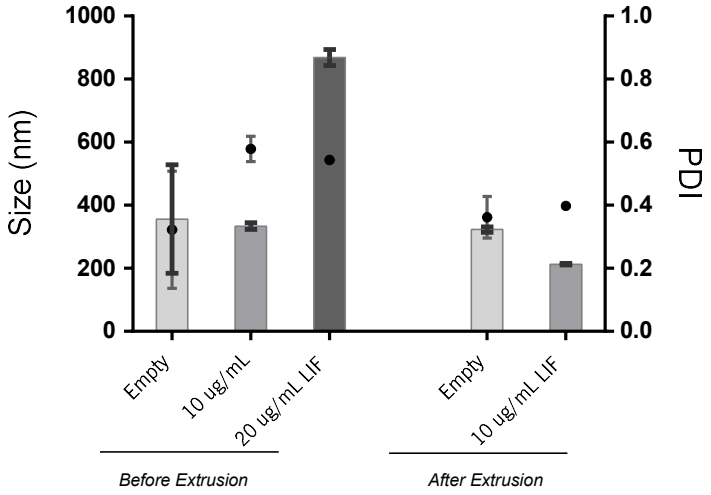

B

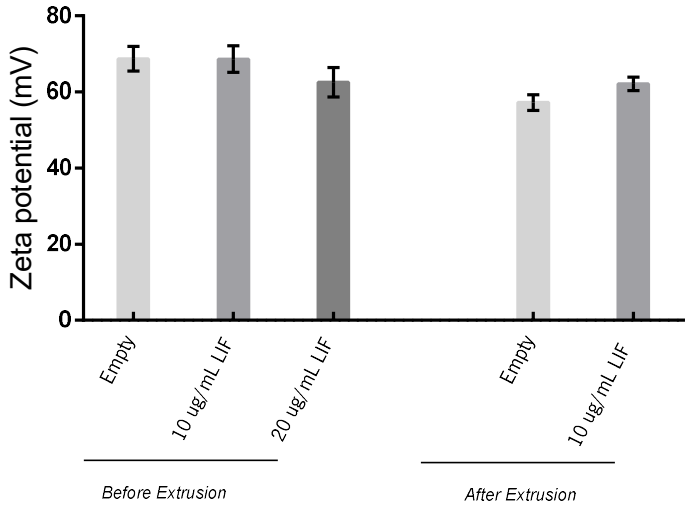

Figure 14 Graphical representation of **A-** size and **B-** surface charge for 0.4mM liposomes encapsulating 10 µg/mL and 20 µg/mL of LIF.

When using 0.4mM DODAB:MO to encapsulate 20 µg/mL of LIF, produced a colloidal solution, possibly composed by protein aggregates that may precipitate **(Fig.15)**.

Figure 15 Colloidal solution resulted from the condition of 0.4mM encapsulating 20 µg/mL of LIF.

This colloidal effect must be due to the lower lipid concentration compared to the quantity of protein to be encapsulated. The ratio from 0.4mM DODAB:MO:10 µg/mL to 0.4mM DODAB:MO:20 µg/mL decreases by half. This means, that this condition, will have more protein for the same quantity of lipid. For 0.4mM DODAB:MO:10 µg/mL condition this effect was not observed, and so the liposomes went through extrusion process. Regarding this latter, it is notice a highly positive charged liposome. This result suggests that most of the related LIF is encapsulated inside the liposomal formulation.

The results demonstrate two extremes of LIF concentration, and for future *in vitro* assays, it was necessary to maintain a low lipid concentration, and decrease LIF concentration as an option. Decreasing LIF concentration, there is more lipid to solubilize the protein.

4.2.2. LIF Encapsulation efficiency

To verify % of LIF encapsulation, the optimized Bradford method used with BSA was used. The calibration curve comprises a range of concentrations between 0.1 and 5 µg/mL **(Fig.16)**.

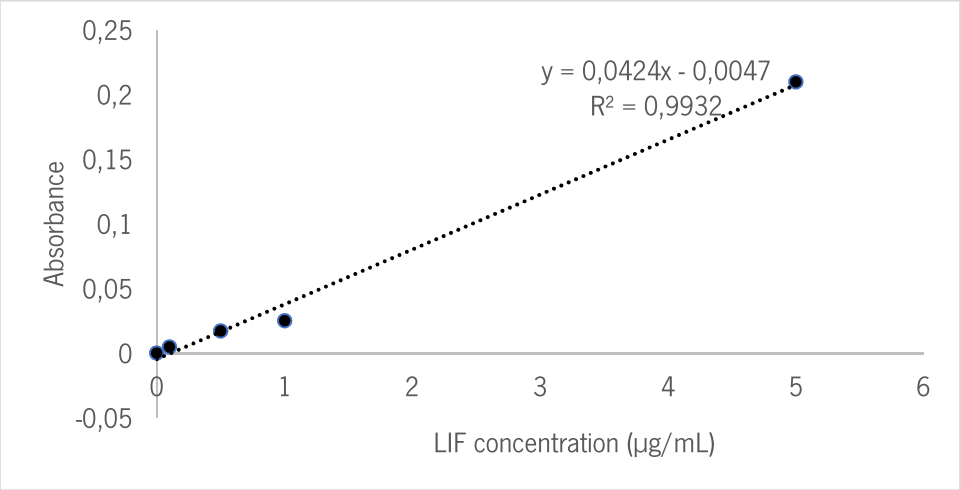

Figure 16 Calibration curve obtained by Bradford method, for encapsulated LIF quantification between 0.1 and 5 µg/mL.

The method was only sensitive until 5 µg/mL of LIF probably because of the higher quantity of LIF in the same volume compared to BSA. Despite BSA had a higher molar concentration, this implies a lower mass concentration, decreasing the number of molecules in the same volume as LIF.

For encapsulation efficiency evaluation it was used the encapsulated portion of the separation process by amicons. Due to protein aggregation, sensitivity to pH and temperature present in some proteins [106] may be important features present in LIF, it was quantified the encapsulated protein and extrapolated the value for a total protein concentration of 5 µg/mL in two independent assays **(Table 8)**.

Table 8 Encapsulation efficiency for 0.2mM 5 µg/mL of LIF formulation (n=2). The t-test was performed: data statistically not significant.

Liposomal formulation	$[LIF]_{Encapsulated}$ (µg/mL)	Standard deviation	Encapsulation Efficiency (%)
0.2 mM 5 µg/mL LIF	4,280	0,036	85,593

Since the sample only had two results to be analyzed, t-test was performed. The data do not show relevant differences between the two results. Using DODAB:MO (1:2) carrier is an advantage to solubilize the protein, and it may prevent the formation of protein aggregates. The encapsulation efficiency was verified by ELISA assay **(Fig.17)**.

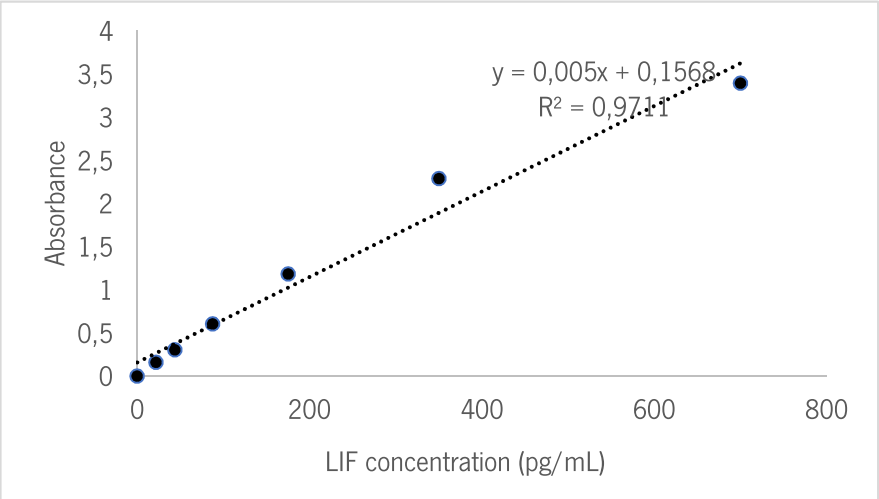

Figure 17 Calibration curve obtained with ELISA kit to quantify murine LIF.

ELISA assay allowed to quantify the encapsulated protein inside the liposomes and extrapolate the results considering as total protein 5ug/mL of LIF. From this, it was obtained a percentage of encapsulation efficiency of approximately 74% **(Table 9)**.

Table 9 ELISA results for quantification of encapsulated LIF inside the core of the liposomes.

Liposomal formulation	[LIF]*encapsulated* (µg/mL)	Encapsulation Efficiency (%)
0.2 mM 5 µg/mL LIF	3.700969	74.019

These results show that these nanocarrier have high encapsulation efficiency. More assays are needed in order to confirm the encapsulation efficiency tendency. Despite that, carriers encapsulate LIF with high efficiency. As LIF triggers response when interacting with the receptor, it needs to be adsorbed in liposome surface and that can be achieved using LIF conjugated with PEG-maleimide. In order to use a system with less lipid concentration, the protein concentrations need to decrease in order to increase the L/P ratio. This means, that using lower protein concentration, without PEG strategy, the protein would be encapsulated and not accessible at the surface. Comparison assays of the two systems, protein encapsulated or at the surface need to be made in order to create an optimal carrier to transport LIF through a biological system.

4.3. Stability assays

4.3.1. DODAB:MO encapsulating BSA

Liposomes encapsulating BSA were produced in 0.4mM lipid concentration and were characterized in terms of size and surface charge **(Fig.18)**.

A

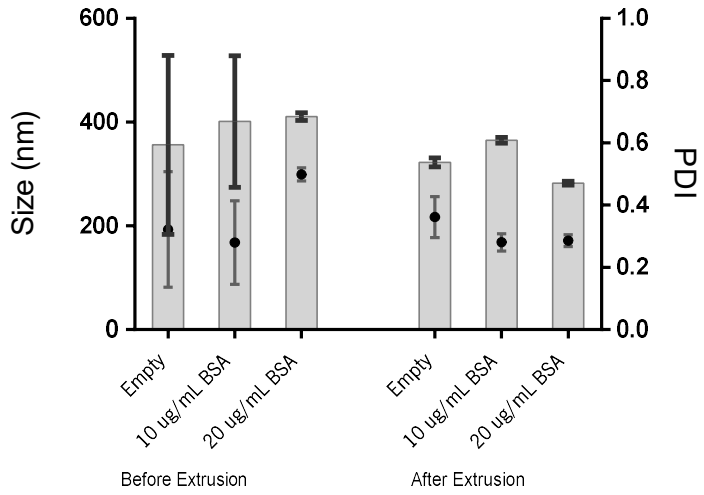

B

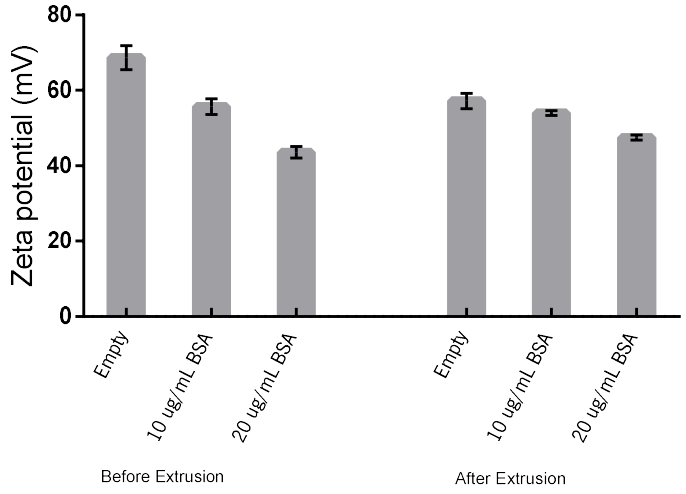

Figure 18 Characterization of **A-** size and **B-** surface charge of liposomes stock solution at 0.4mM encapsulating 10 and 20 µg/mL of BSA.

Liposomes DODAB:MO (1:2) prepared using 0.4mM lipid concentration after extrusion are very similar in size and the surface charge remained positive, compared with liposomes before extrusion. Because of that, this lipid concentration was chosen to be the stock solution and was diluted 1:2 to reach a final lipid concentration of 0.2mM. Liposomes were diluted in: HEPES solution at pH 5; HEPES solution at pH 7.4; and 25% of FBS. Dilutions were needed because it was not possible to do continuous read. As

an example, a continuous curve can be created in which liposomes were exposed to different pH and evaluated in terms of size and surface charge, but the final lipid and protein concentrations wouldn´t be the same as the initial.

The stability for 0.2mM DODAB:MO (1:2) was evaluated during 6h [86], in intervals of 1h , and with an extra analysis at 30 min. The average size and surface charge were analyzed **(Fig.19 and 20)**, although for a more specific information of stability the mean percentage of populations present in the sample was considered **(Supplementary material)**.

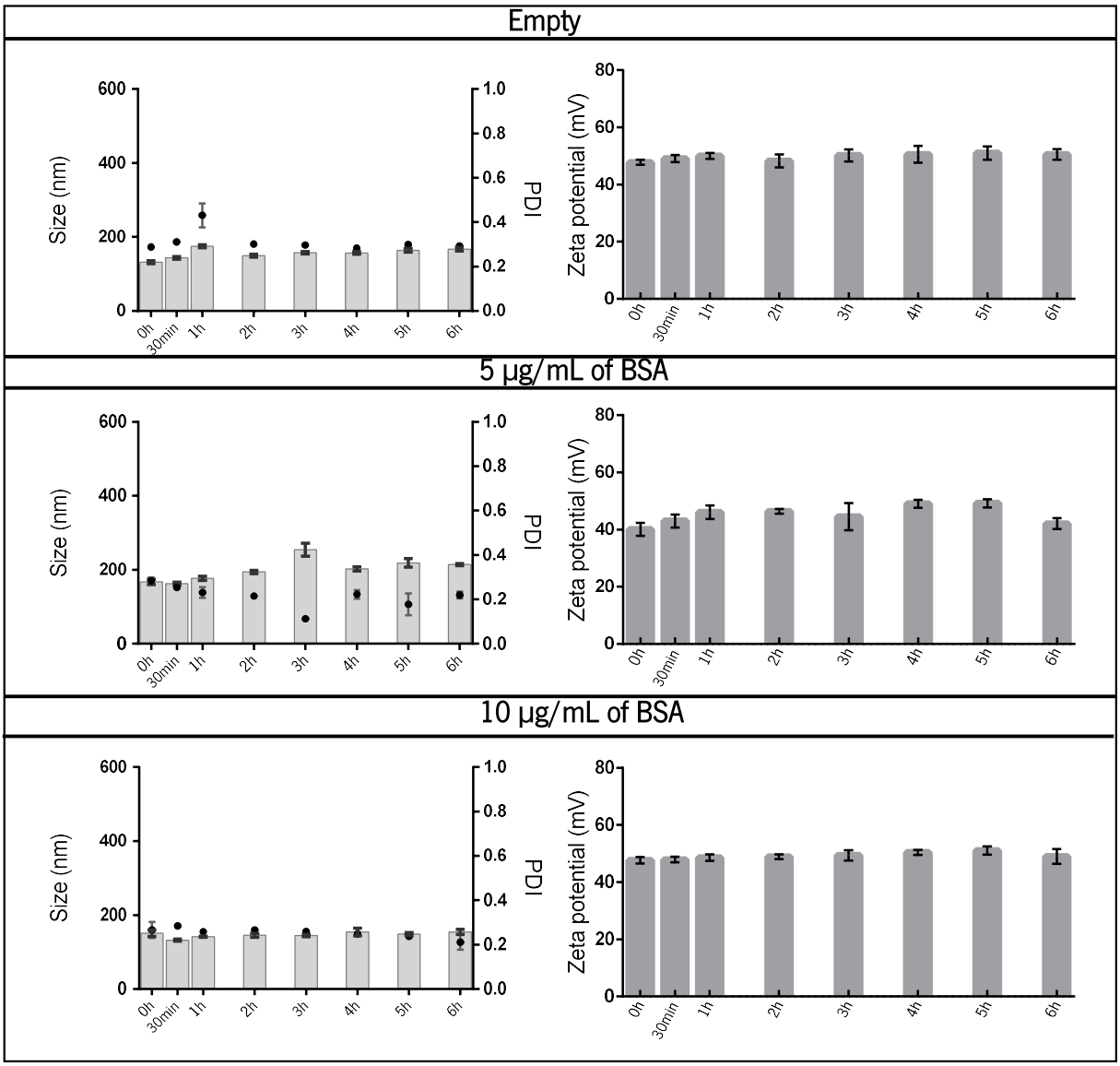

Figure 19 Results from stability for DODAB:MO liposomes empty and encapsulating 5 and 10 µg/mL of BSA at pH 5.

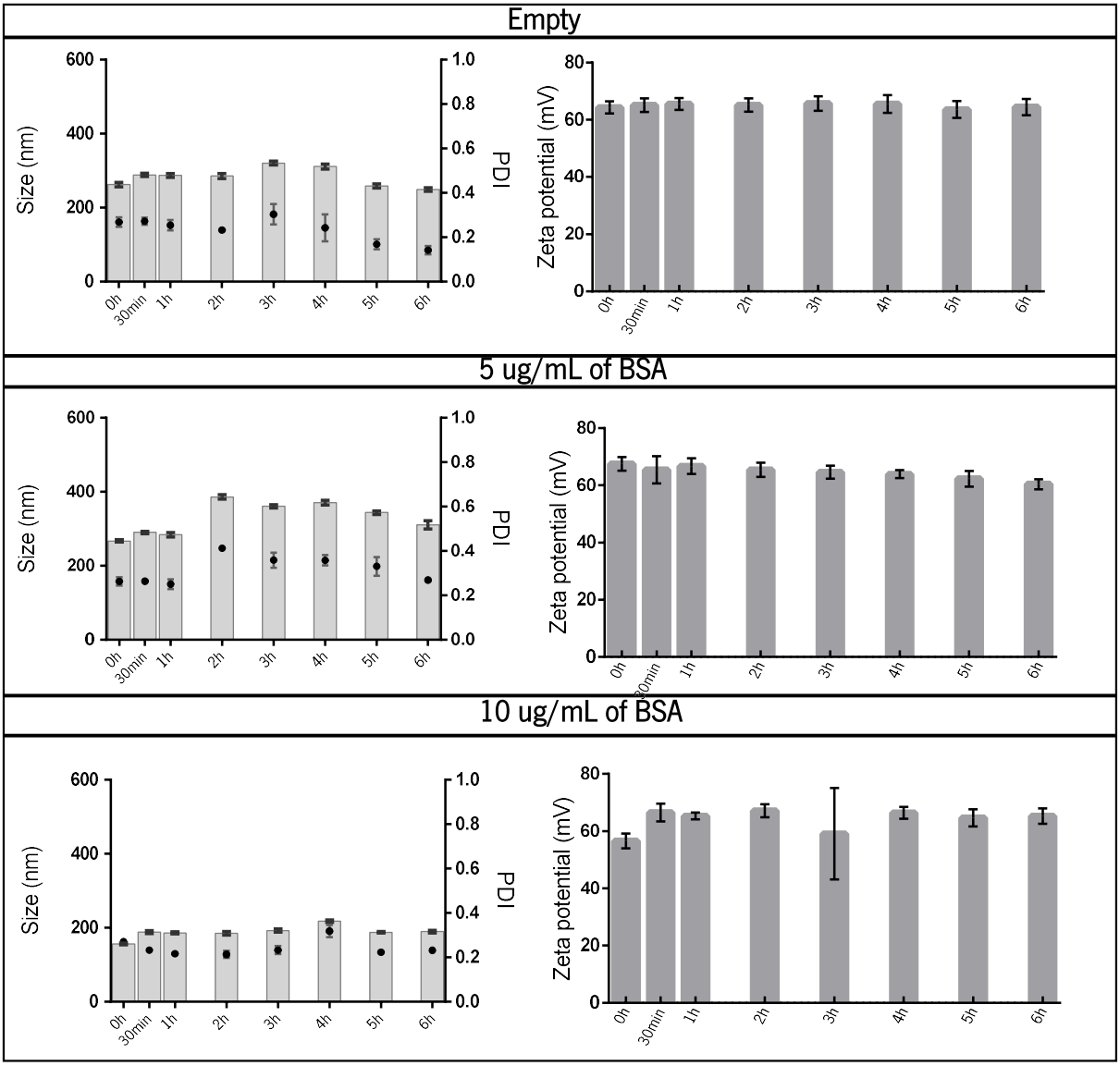

Figure 20 Results from stability for DODAB:MO liposomes empty and encapsulating 5 and 10 µg/mL of BSA at pH 7.4.

Regarding size and surface charge results for HEPES solution in pH 5 and 7.4, it is demonstrated a hydrogen ions (H^+ ions) effect in liposomes packing. The solution with acidic pH is rich in H^+ ions and consequently, the equilibrium of the liposomal structure resulting from repulsion forces between the heads is destabilized. The positive charge of the hydrogen ions interacts with the surface of the liposome increasing the repulsion between the lipid heads and consequently decreasing the liposomal structure size.

Despite of that, the results indicate an increase in stability at pH 5 because of the reduced number of populations when liposomes encapsulate BSA **(Supplementary Material)**. About stability in 25% of FBS, the proteins in the serum may bind to the liposome surface and neutralize the charge **(Fig.21)**.

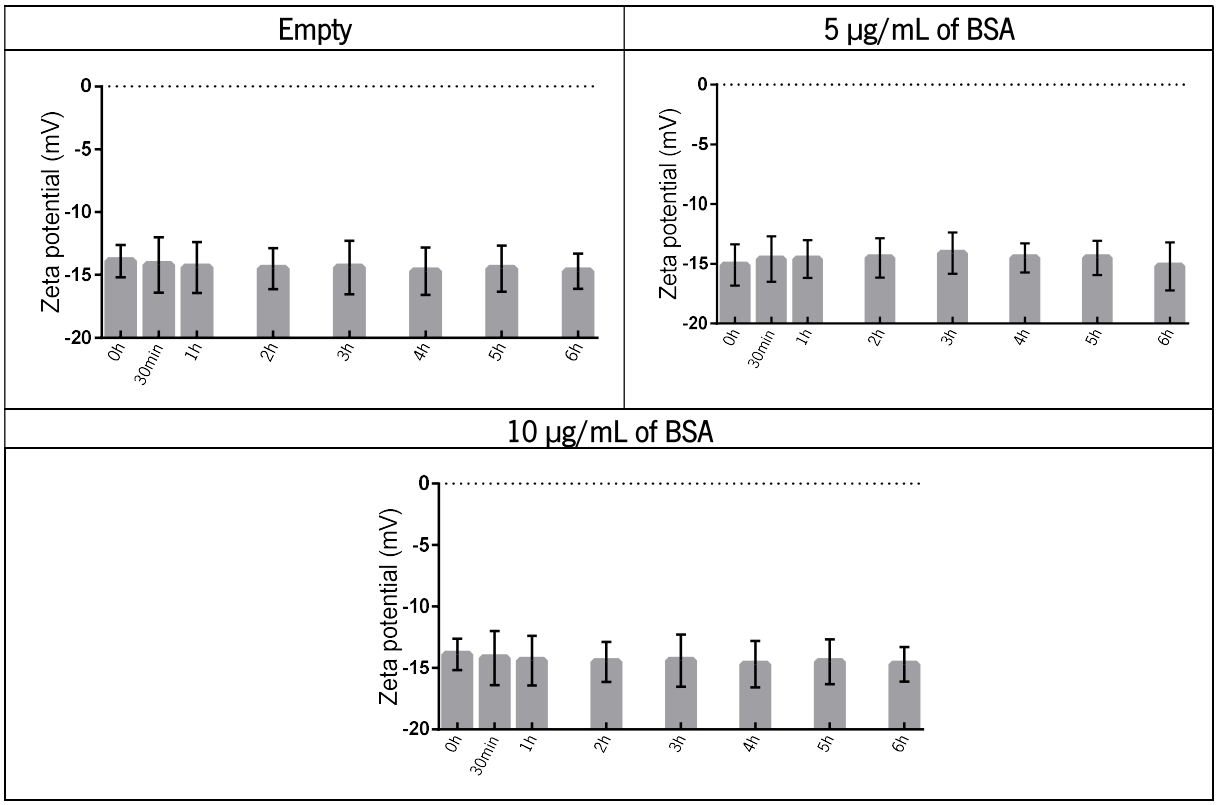

Figure 21 Surface charge analysis in 25% of FBS of liposomes encapsulating BSA.

Liposomes in 25% of FBS are very unstable. Not only, the serum proteins may bind to the surface but also the balance of forces that maintain the structure is destabilized. The serum is composed by several proteins that may have charged amino acid residues being possible the formation of aggregates by electrostatic interactions. Due to that fact, the number of populations increases producing an index of polydispersity close to one (Fig.22).

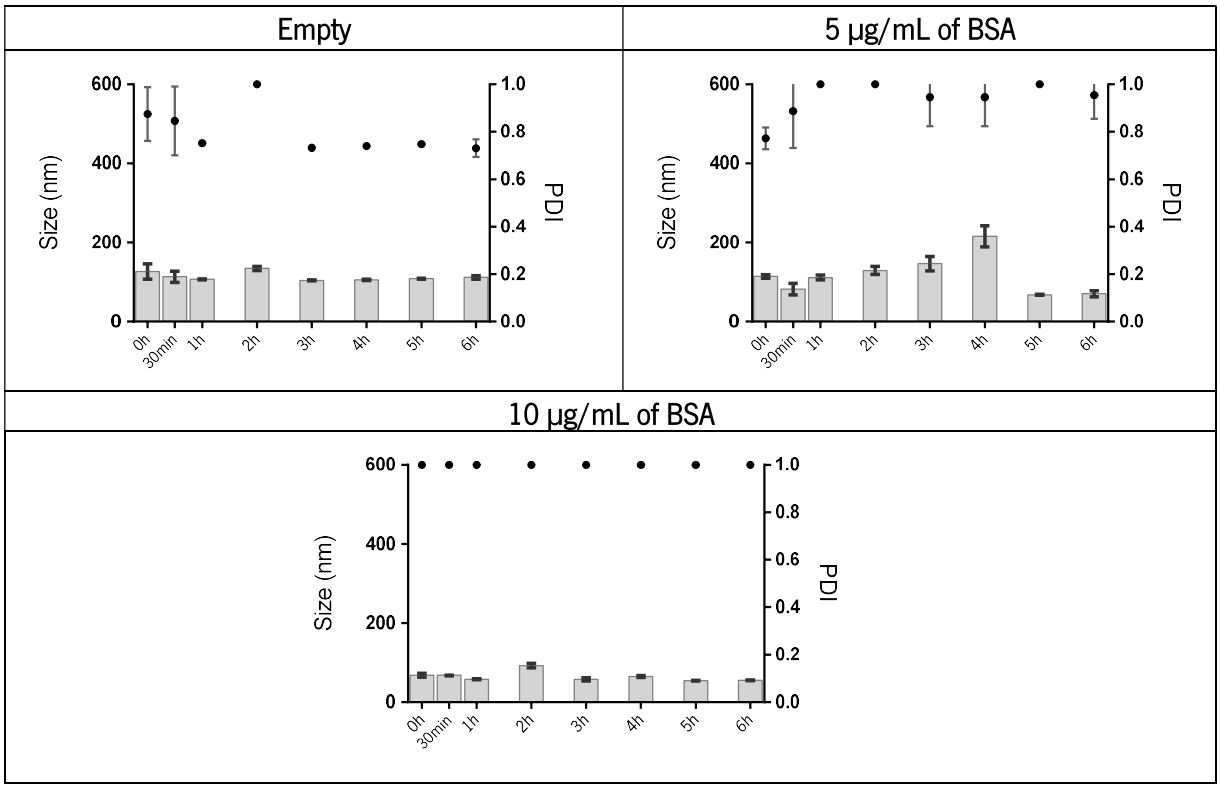

Figure 22 Size measurements from DODAB:MO encapsulating BSA in 25% of FBS.

In summary, liposomes DODAB:MO (1:2) encapsulating BSA are stable at pH 5 due to the packing effect. At pH 7.4 the size increases because of the presence of OH^- ions. These ions neutralize the positive charge on the liposome surface and the structure destabilizes, slightly increasing the size. When exposed to 25% of FBS, serum proteins may be destabilizers of this cationic liposomes. Negative charged proteins can bind to the positive surface decreasing the surface charge and interfering in the electrostatic forces that holds the structure together.

4.3.2. DODAB:MO encapsulating LIF

For stability assays only, the condition 0.4mM DODAB:MO 10 µg/mL LIF was analyzed. After dilution 1:2, the liposomes were at 0.2mM DODAB:MO 5 µg/mL of LIF. The same solutions of HEPES at pH5 and 7.4 and 25% of FBS were used. Size **(Fig.23)** and Surface charge **(Fig.24)** were measure in order to understand the stability of these liposomes.

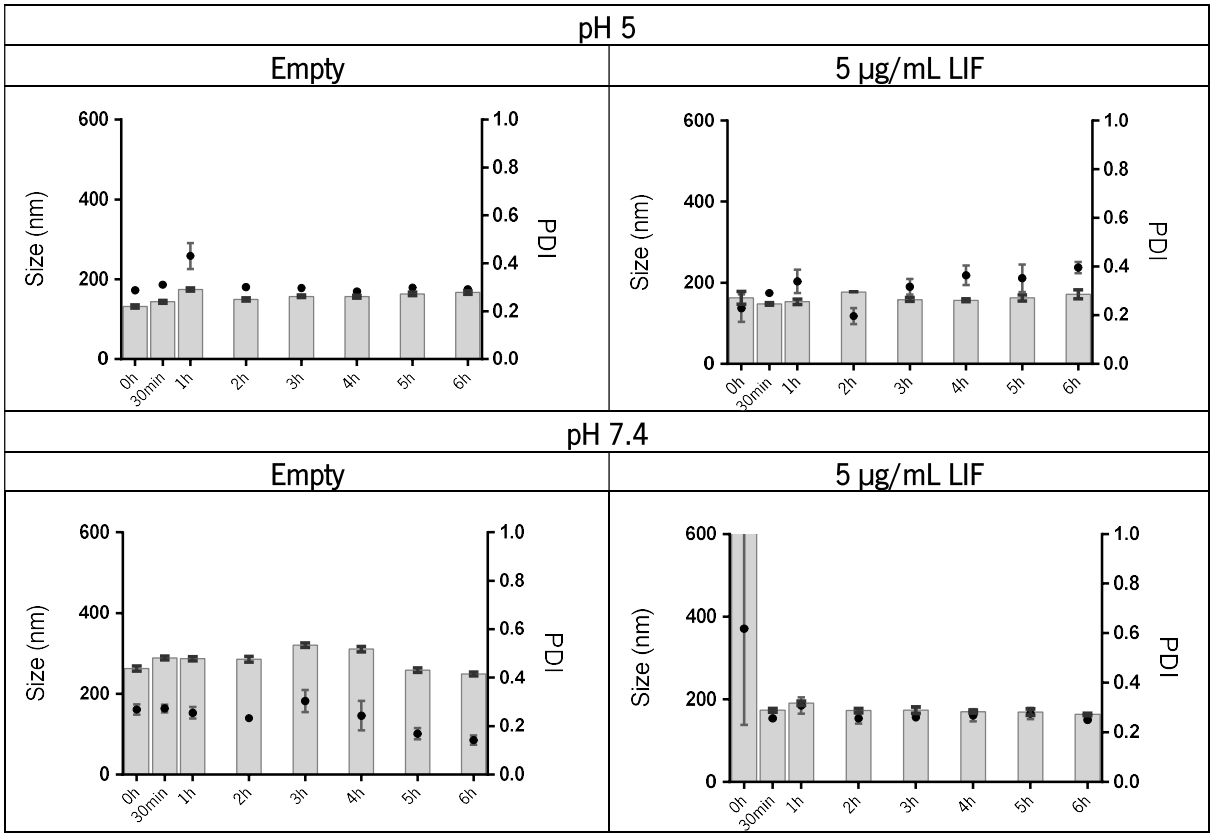

Figure 23 Size measurements of DODAB:MO carriers encapsulating LIF at pH 5 and 7.4.

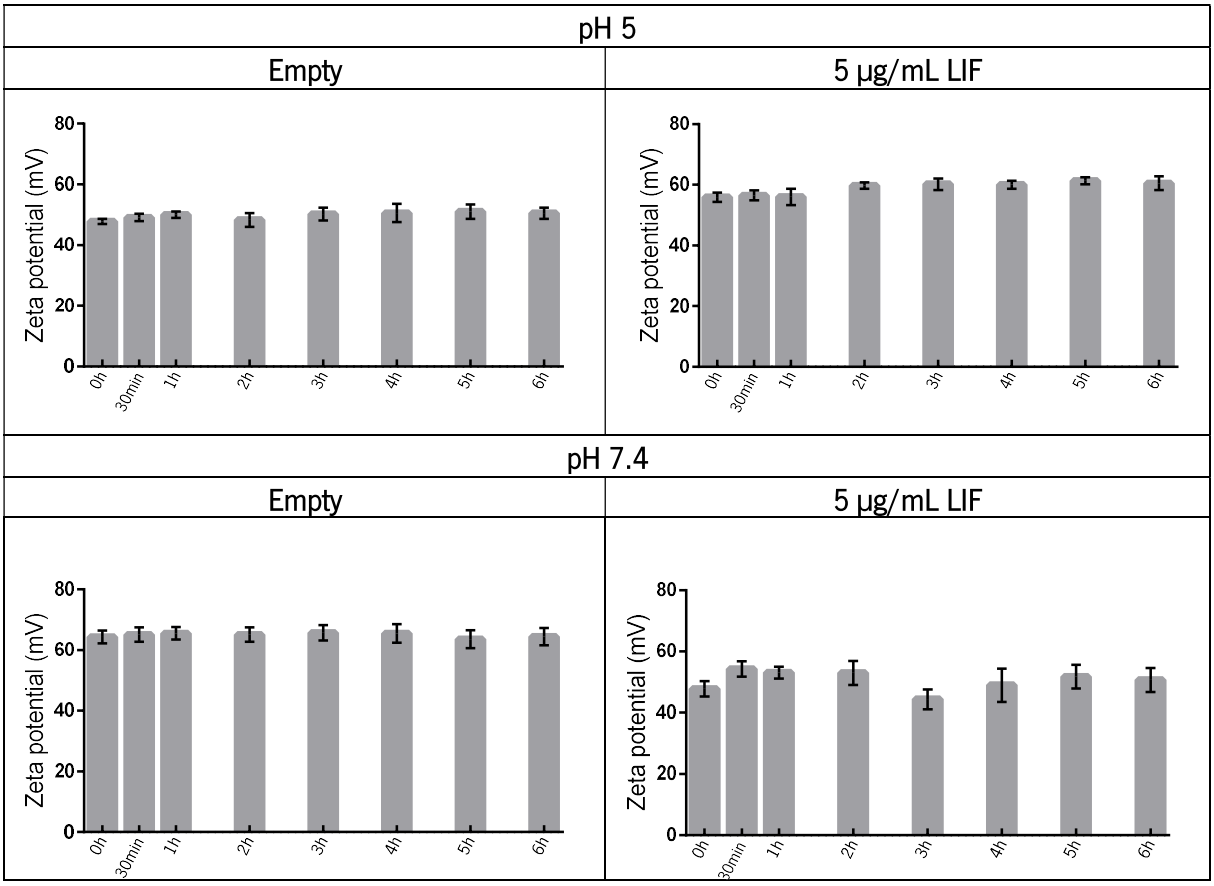

Figure 24 Surface charge measurements of DODAB:MO carriers encapsulating LIF at pH 5 and 7.4.

Liposomes DODAB:MO encapsulating LIF are very positive demonstrating to be stable at pH 5 and 7.4. The size did not decrease when liposomes were exposed to pH 5, because despite of the increased H^+ ions in the medium, they are very positive charged. Also, the ions OH^- were not capable of increasing the size of the liposome by neutralizing the charge at the surface. When exposed to 25% of serum liposomes destabilize, increasing in size and becoming negatively charge possible due to serum proteins binding **(Fig.25)**.

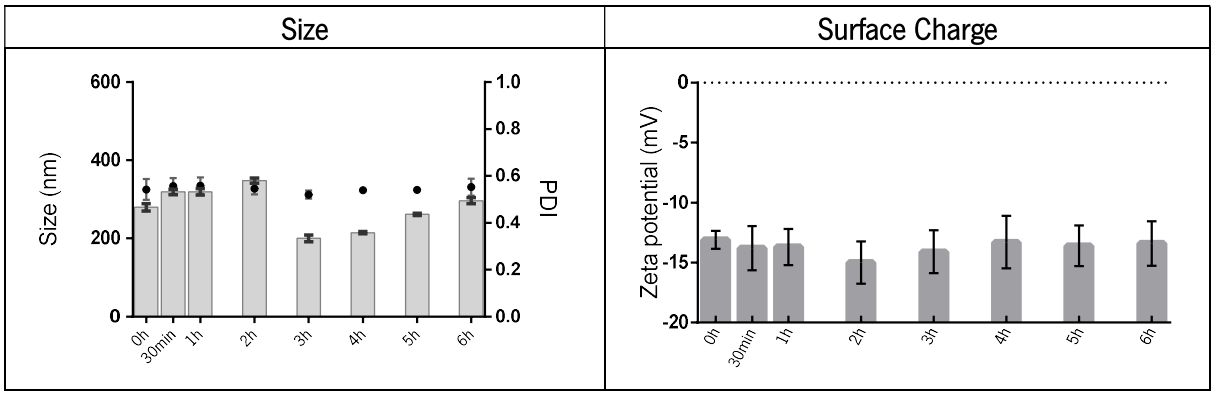

Figure 25 Surface charge and size measurements of DODAB:MO carriers encapsulating LIF when exposed to 25% of FBS.

4.4. Toxicity of DODAB:MO (1:2)

The toxicity for both DODAB:MO (1:2) and novel liposomes was analyzed using hemolysis. This method detects the release of hemoglobin from red cells when disrupted if the nanoparticle is toxic to them, leading to a more intense red color in solution **(Fig.26)**. The results from two independent assays were analyzed and are illustrated in **figure 27**.

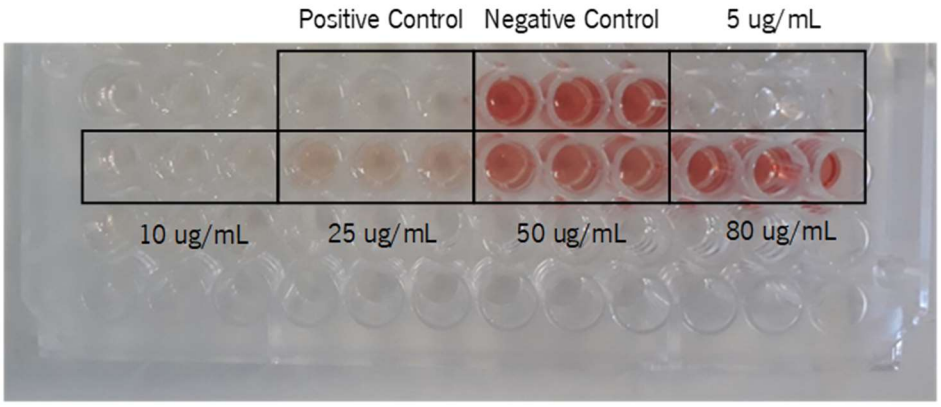

Figure 26 Plate from hemolysis assay with DODAB:MO (1:2), demonstrating the increased red color while lipid concentration became higher.

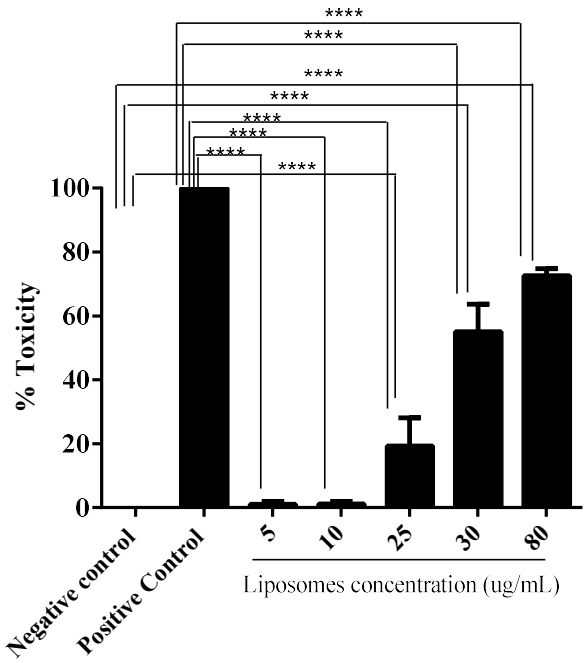

Figure 27 Absorbance regarding hemolysis assay of DODAB:MO (1:2) carriers, which are toxic for concentrations between 25 and 80 μg/mL (n=2). Results statistically analyzed by ANOVA (Tukey´s test) ($\alpha \leq 0.05$).

The results considered statistically relevant by ANOVA test are represented in the graph. This means that the highlighted results in asterisk, if the assay is repeated, there are lower probability to have no differences between the conditions. DODAB:MO (1:2) liposomes toxicity is more accentuated in higher lipid concentrations, such as 25, 50 and 80 μg/mL. For future applications *in vitro* or *in vivo*, lower concentrations of this nanocarrier are more suitable in order to have lower toxicity.

5. Cell culture assays

5.1. C2C12 cell line

5.1.1. Proliferation assays

C2C12 cells are myoblasts and the presence of LIF is described in the literature as a proliferation stimulator, delaying differentiation for concentrations below 0.01 ng/mL [35]. The results from the proliferation assays conducted in this subchapter were normalized relatively to the control condition, which was considered as 100% of cell proliferation. For proliferation assessment, the SRB assay was firstly used. In this one independent assay, the three LIF concentrations (0.01;0.1;1 ng/mL) were analyzed. The respective obtained results are presented in the following figure **(Fig.28)**.

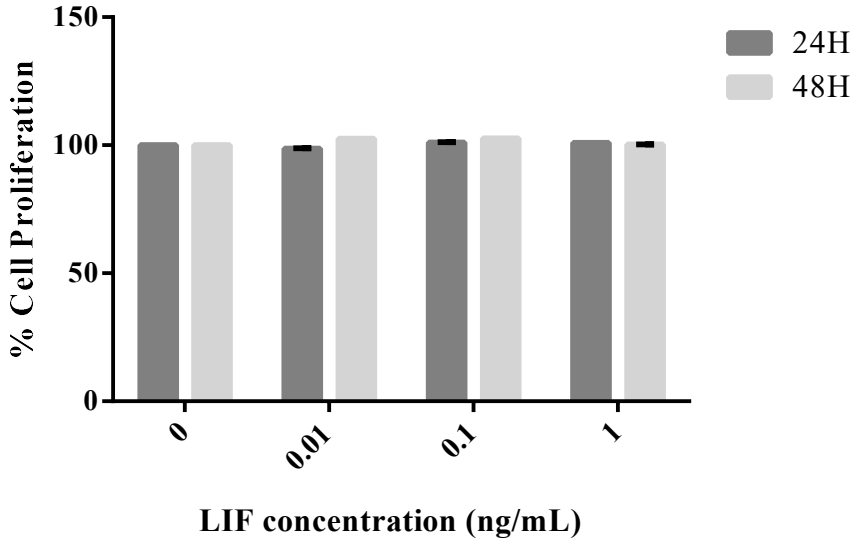

Figure 28 Results from the proliferation assay with SRB, where C2C12 cells were seeded at $2x10^5$ cells/mL and exposed to different concentrations of LIF. There are no significant differences between concentrations and timepoints (n=1).

There are no evident differences in proliferation for the distinctive concentrations, even when the assay is conducted for 48h. Because of these results and knowing the highly proliferative characteristic of the myoblast cell line, the cell density was reduced for $1.25x10^5$ cells/mL (one independent assay) **(Fig.29)** and an additional assay was performed.

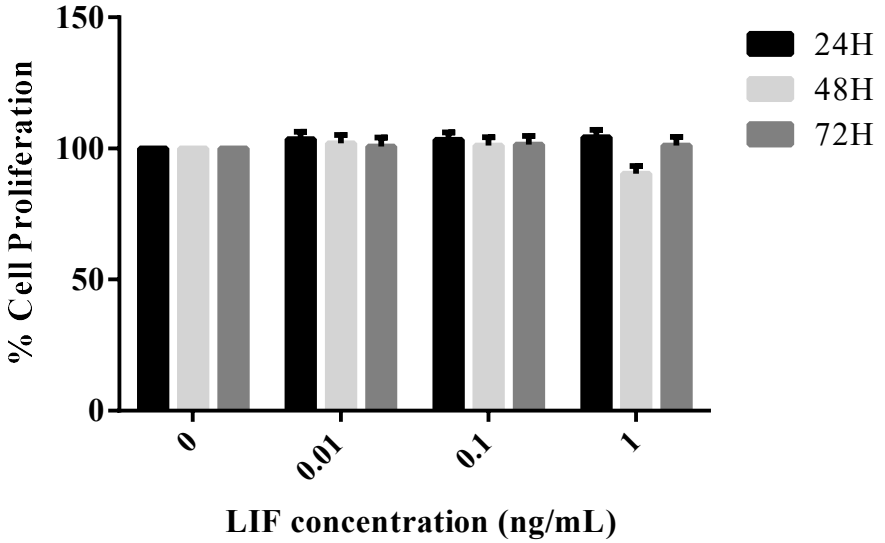

Figure 29 Results from the second proliferation assay with SRB, where C2C12 cells were seeded at $1.25x10^5$ cells/mL and exposed to different LIF concentrations. The expected proliferative state at 0.01 ng/mL was not evident regardless of the timepoints (n=1).

The SRB assay is directed to protein quantification and extrapolation for mass quantity, although muscle cells are producers of several specialized proteins. Therefore, the signal can be saturated and provide a false positive for proliferation rates.

The Hoechst assay, as this probe detects DNA and consequently can extrapolate the results for cell number, after an initial seeding of $1x10^5$ cells/mL **(Fig.30)**. For this one independent assay, only the 0.01 ng/mL concentration of LIF, described as the concentration with which myoblasts reach the maximum proliferative state, was evaluated.

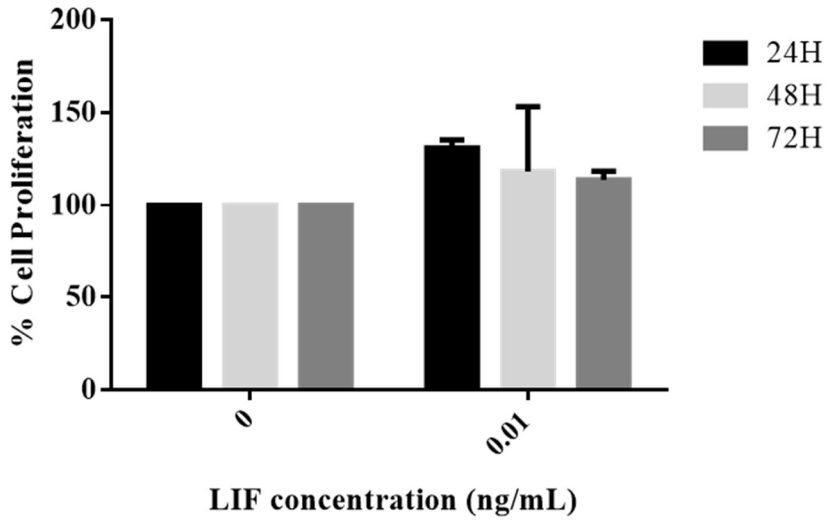

Figure 30 Hoechst assay for C2C12 cells seeded at $1x10^5$ cells/mL and exposed to 0.01 ng/mL LIF. The reduced density demonstrated to be important to assess the proliferative response of myoblasts for a longer assays up to 72h (n=1).

Reducing cell density demonstrated to be important for properly assessing cell response to LIF stimulation. When cells were seeded with lower density and the assay reached 72h without visible cell aggregation in the culture (Fig.31). It is identifiable an increase of proliferation rate of almost 50% at 24h comparing to the control. After, the proliferation rate seems to decrease but being higher than the control, may be due to differentiation.

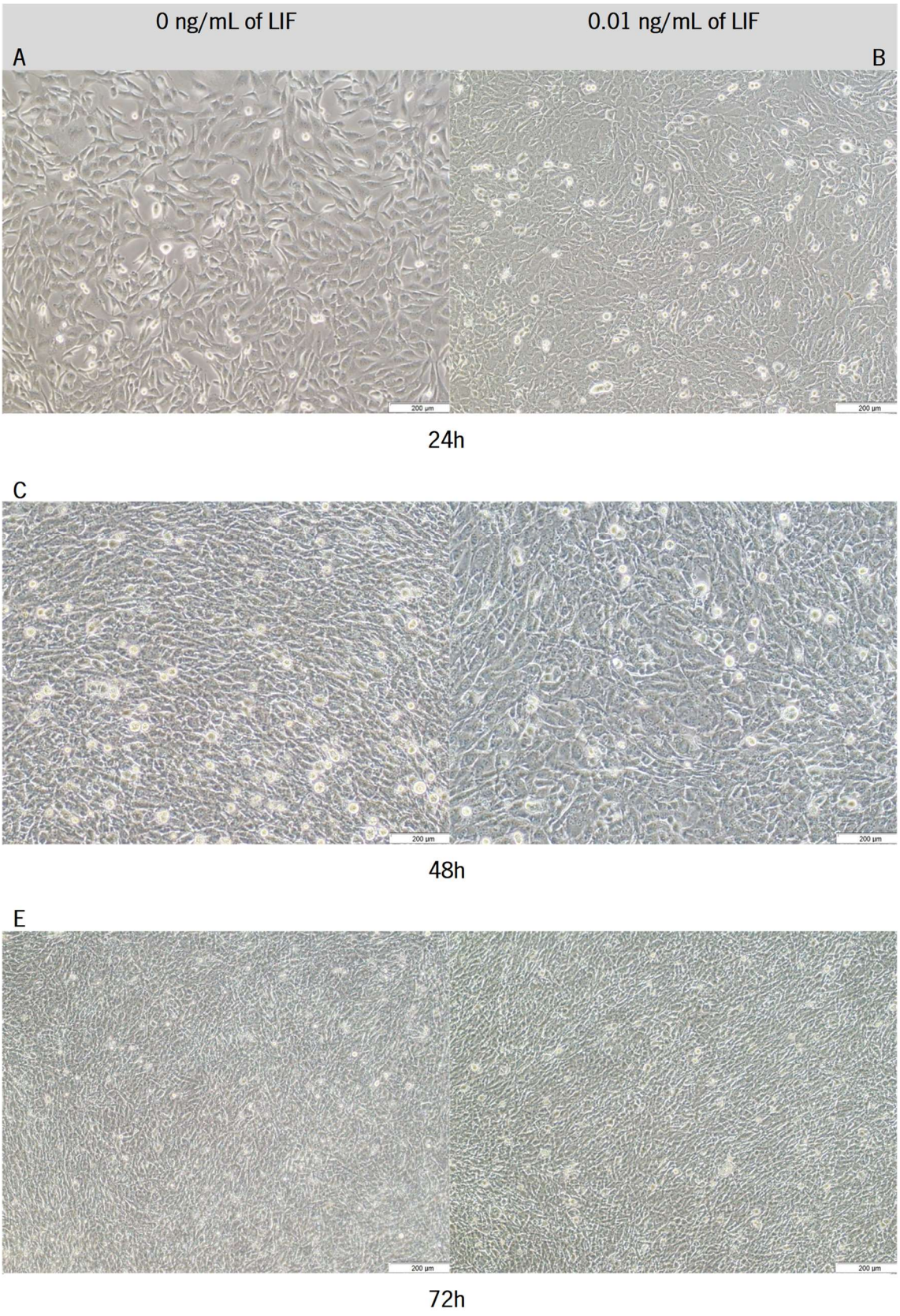

Figure 31 C2C12 cells seeded at $1x10^5$ cells/mL and grown in different conditions up to 72h **A; C; E** without LIF and **B; D; F** with 0.01 ng/mL. Bright field (100x). Scale bar: 200 µm. Records obtained through inverted Fluorescence Microscope.

Observing the images, it is noticeable an organization and an orientation of the cells, phenomenon related to the beginning of differentiation.

Respecting the proliferation results, where results of LIF at 0.01 ng/mL where observed, cell density appears to be important to evaluate proliferation. Because of that, another assay was conducted, with cell density reduced to $1x10^4$ cells/mL and the three LIF concentrations (0.01, 0.1 and 1 ng/mL) were analyzed for five days **(Fig.32)**.

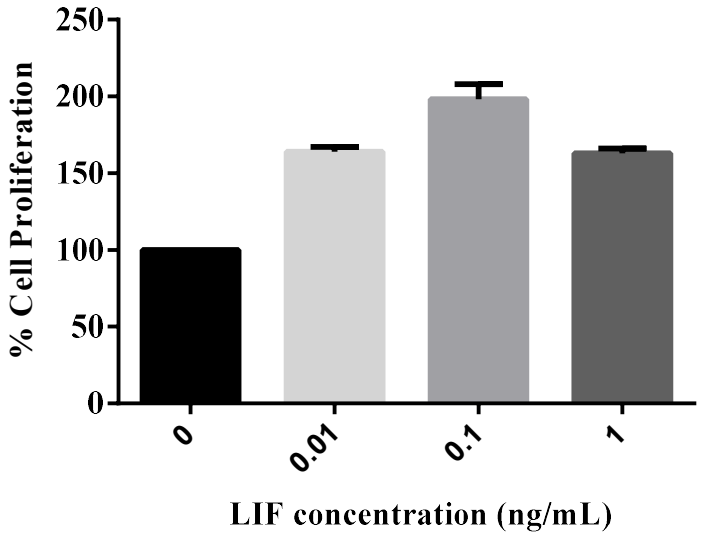

Figure 32 Results of the Hoechst assay applied to C2C12 cells seeded at $1x10^4$ cells/mL and stimulated with LIF concentrations: 0.01, 0.1 and 1 ng/mL. The reduced initial seeding cell density reveals the difference obtained with LIF concentrations (n=1).

The results showed significant differences in cell response obtained with varying concentrations, with an increasing effect from 0 to 0.1 ng/mL and a decrease in proliferation with for 1 ng/mL LIF. Despite being described in the literature that the 0.012 ng/mL of LIF has the greater proliferative effect [35], in this assay 0.1 ng/mL concentration demonstrated to be more effective for proliferation stimulation. With this concentration the cells proliferate 100% more compared to the cells without LIF treatment. When the concentration increase for 1 ng/mL, the rate of proliferation slightly decreases. This indicate that there is a peak of maximum response for proliferation at low concentrations of LIF.

In order to continue the assays, more replicas are needed with 0.01 and 0.1 ng/mL concentrations as the targets to be optimized. Chosing these concentrations, it was important to reach the maximum proliferation rate without differentiation inhibition. Neverthless, the concentration needed for myoblasts proliferation is still low, and a controlled release is an option. This effect can be achieved with a nanocarrier encapsulating the protein.

5.1.2. Differentiation assay

The differentiation assay was made in order to verify which horse serum (HS) content in the culture medium percentage (2 or 5%) is more adequate to induce differentiation after seven days. Despite LIF is used to promote proliferation, differentiation needs to be stimulated after LIF effect in order to produce myotubes. One independent Hoechst assay was performed to confirm if cells were proliferating or not **(Fig.33 and 34)** and eosin and hematoxylin staining was also performed to determine the presence if differentiation occurred by detecting the presence of myotubes **(Fig.35)**.

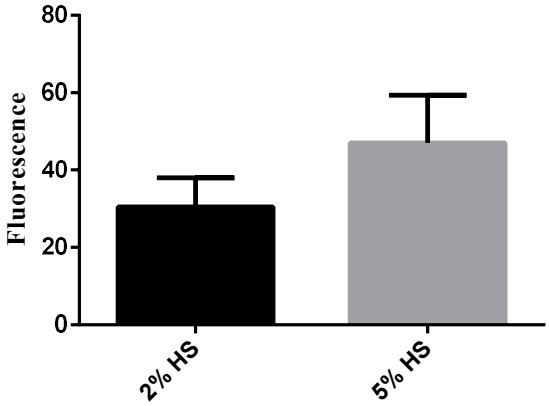

Figure 33 Hoechst assay of C2C12 cells grown with different percentages of HS showed more proliferation with 5%HS (n=1).

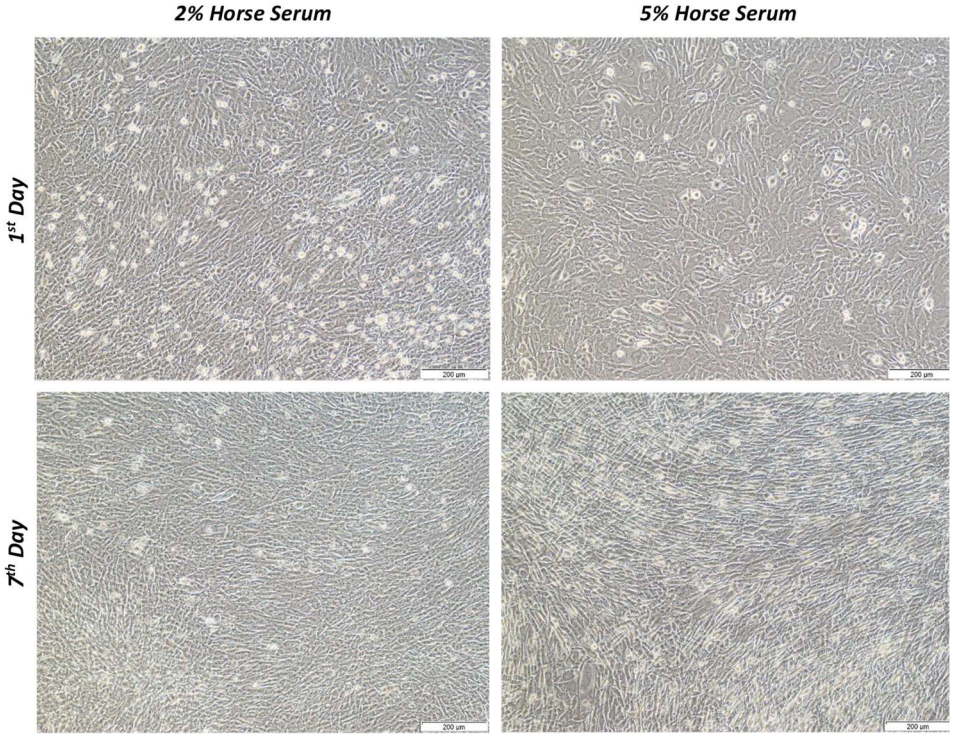

Figure 34 Morphology of C2C12 cell differentiated for 7 days with medium containing different contents of HS. Bright field (100x). Scale bar: 200 µm. Records obtained through inverted Fluorescence Microscope.

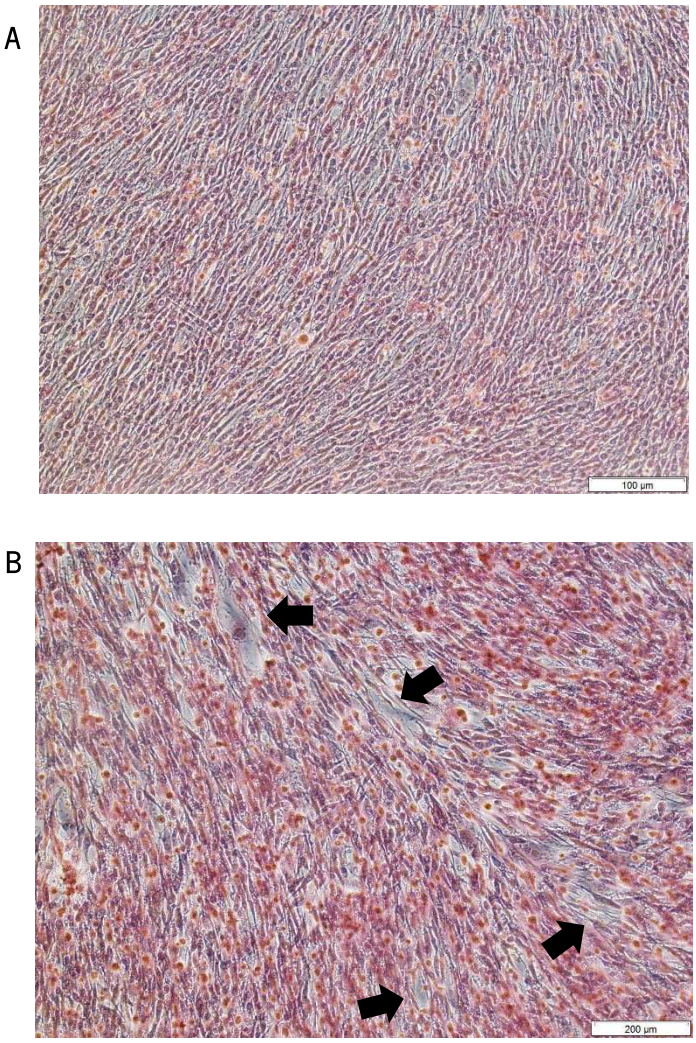

Figure 35 Hematoxylin-Eosin staining of **A-** C2C12 cells induced to differentiate with 2%HS, **B-** cells induced to cultured with 5%HS. The latter differentiated sooner as is visible with presence of wider caliber myotubes (black arrows). Bright field (100x). Scale bar: 200 µm. Records obtained through inverted Fluorescence Microscope.

The HS stimulates cells to proliferate and differentiate and the highest concentration of HS boosted proliferation and an early differentiation. In assays dependent on LIF treatment, the horse serum can mask the proliferative effect of the cytokine. On the other hand, if the intended result is differentiation using 5% HS have a synergic effect with LIF.

5.2. M1 cell line

5.2.1. Proliferation assays

In order to evaluate proliferation in M1 cells, the Hoechst assay was performed. Five different concentrations were analyzed (0.001;0.01;0.1 ng/mL) [19] and the results are represented in **figure 36**. Two independent assays, spanning five days were performed.

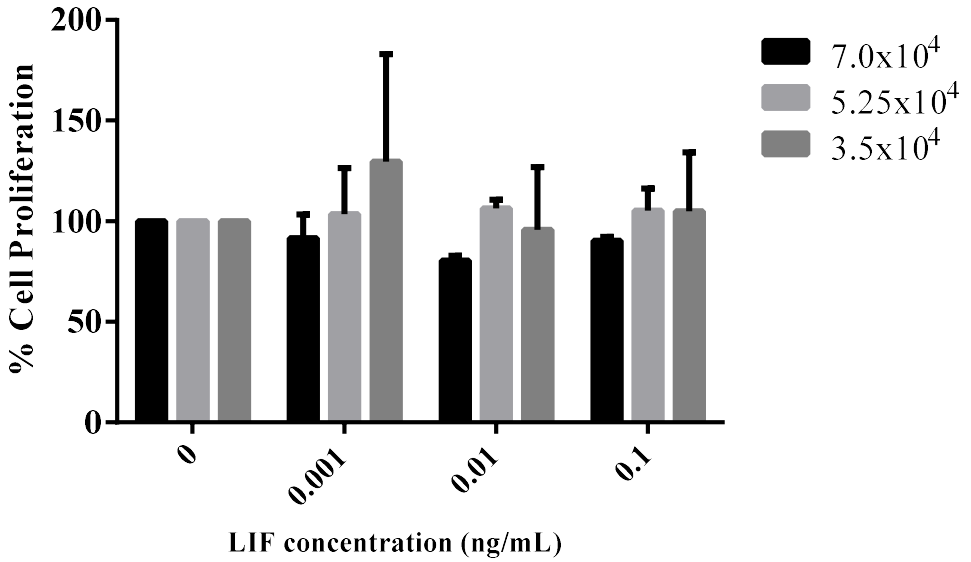

Figure 36 Hoechst assay results for proliferation evaluation of M1 cells cultured for five days with medium containing LIF stimulation at concentrations of 0.001; 0.01 and 0.1 ng/mL for five days. There are no significant differences between concentrations despite the different cell density. Two-way ANOVA (Tukey´s test) was performed, and the data was not statistically significant (n=2).

The data were statistically analyzed with ANOVA test and they were considered not statistically relevant. This means that the data does not demonstrate to have significant differences among the conditions. According, to the literature, M1 cells have an EC_{50} of 0.2 ng/mL of LIF, this means that at this concentration, 50% of the cells are inhibited from growing [19]. This phenomenon is not observed in this data. If LIF increases, the cell response remains almost unchanged, despite the decrease in cell density. Despite the lack of statistical significance, with $5.25x10^4$ cells/mL density or the lowest cell density ($3.5x10^4$ cells/mL), there is a slightly increase in proliferation between 0 and 0.001 ng/mL, followed by a decrease in proliferation for 0.01 and 0.1 ng/mL LIF concentrations.

LIF can lose activity if storage is longer than three months, and this is a factor that can influence the expected function of LIF in cells. For validation of the cell line and dose-dependent responses to LIF concentrations other assays with other commercial LIF protein should be made.

5.2.2. Viability assay

The cells viability was analyzed by trypan blue assay (two independent assays) for five days in the same concentrations as above referred: 0, 0.001, 0.01 and 0.1 ng/mL of LIF **(Fig.37).**

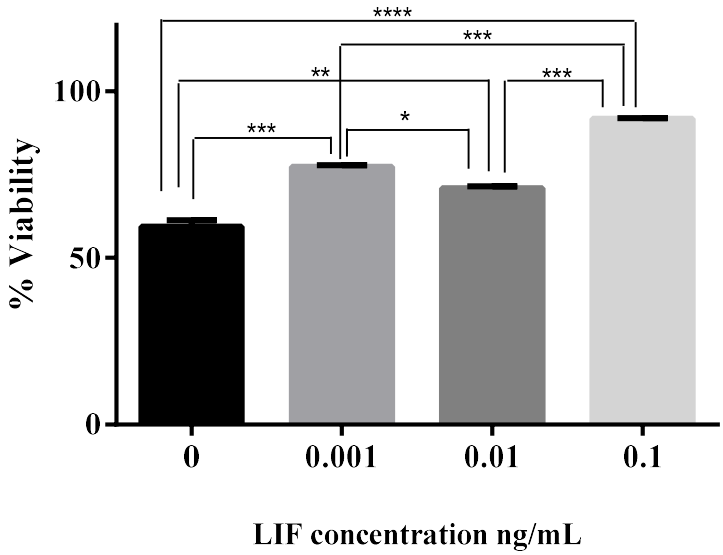

Figure 37 Results from trypan blue applied to C2C12 cells grown for five days (n=2). The results were analyzed by One-way ANOVA (Tukey´s test): $P < 0.0001$.

Evaluating the results figure 38, LIF seems to increase cell viability, meaning that it is not toxic for M1 cells. Nevertheless, a notorious effect would depend on LIF concentration. For 0.1 ng/mL LIF, the viability increased almost 50% compared to the 0 ng/mL condition and approximately 30%, compared to the 0.001 and 0.01 ng/mL conditions. One-way ANOVA was performed, and there is a 0.0001% of probability, that if the assay is repeated, no differences will be seen between the conditions.

According, to the discussed proliferation results, lower rates of proliferation induced by 0.1 ng/mL of LIF, allow higher cell membrane viability. Lower concentrations are used in cells (nanograms), and because of that a controlled release, which can be achieved with a DODAB:MO carrier, is important to ensure differentiation of M1 cells.

6. Conclusions

The main goal of this work was to encapsulate LIF in DODAB:MO (1:2) carrier and validate this nanosystem in relevant cell models.

In order to optimize the concentrations of lipid and LIF, two DODAB:MO (1:2) concentrations (1mM and 0.2mM) and 5 and 10 μg/mL of BSA were used to produce nanocarriers and after characterization in terms of size and surface charge, they did not show significant differences between the two lipid concentrations tested. The nanocarriers were positively charged, regardless of being empty or encapsulating BSA. These results are consistent with an efficient solubilization of BSA inside the DODAB:MO formulation, due to the presence of inverted non-lamellar phases of MO inside. Another goal was to quantify the encapsulated BSA using two different methods, Bradford method and by FITC-BSA fluorescence. The encapsulation efficiency of BSA for 1mM DODAB:MO (1:2):10 μg/mL BSA, 0.2mM DODAB:MO (1:2):5 μg/mL BSA and DODAB:MO (1:2):10 μg/mL BSA were ~94%, ~82 and ~88%, respectively. Having in mind *in vitro* studies, lower lipid concentrations (0.4mM) and 10 and 20 μg/mL of LIF were chosen to avoid cytotoxicity. Due to the lower molecular weight of LIF (~20kDa) compared to BSA (~67kDa), the values of Lipid/Protein (L/P) molar ratio using the same lipid concentration (0.2mM), were quite different, meaning that, for the same lipid concentration, more LIF molecules must be solubilized compared with BSA. The Lipid/Protein molar ratio (L/P) for 0.4mM:10 μg/mL formulation of LIF is lower (800) comparong with BSA (2666.7). For 0.4mM:20 μg/mL of LIF, the L/P is lower (400), compared with BSA (1320). The nanocarrier produced using 0.4mM:10 μg/mL of LIF demonstrated to have a good encapsulation efficiency (~85,8%), good stability at different pH conditions (pH 5 and 7.4) and being positively charged (60-70mV). Therefore, decreasing the Lipid/Protein molar ratio until 800, it was still possible to produce a suitable formulation. The condition with lower L/P ratio (400) from the condition 0.4mM:20 μg/mL of LIF, showed a colloidal behavior, possibly reflecting the lower lipid concentration available to solubilize the protein. It will be necessary to decrease protein concentration and maintain lipid concentration. After the optimal carrier being produced, two cellular models, C2C12 and M1 cell lines, were chosen to validate this nanosystem.

This cell lines were chosen based on the measureable effects triggered by LIF (proliferation and differentiation). C2C12 cell line are immortalized myoblasts that are characterized as potential targets of LIF stimulation. In the literature, it is described that LIF at 0.0012 ng/mL of concentration is a potential proliferation stimulator and it can delay differentiation. Nevertheless, in the performed assays, two concentrations were highlighted (0.001 and 0.1 ng/mL) as promoters of a maximum proliferative effect.

Also, cell density seems to influence the proliferative response and throughout optimizations, the appropriate cell density to conduct proliferation assays in C2C12 was defined to be $1x10^4$ cells/mL. C2C12 myoblasts can be stimulated to differentiate with medium containing HS. The best percentage of HS is dependent on the type of assay that will be performed. A higher percentage of HS influences not only proliferation rates but also induces differentiation. In these assays where proliferation is important, 2% of HS can be the best option. Because C2C12 cells grow superimposed, the methods to assess proliferation and cytotoxicity must be carefully considered.

M1 cell line are myeloblasts from murine myeloid leukemia. Focusing on the proliferative effects, 0.2 ng/mL is the LIF concentration established in the literature, where 50% of the cells are prevented from dividing. The performed assays did not confirm the literature statement, but a decrease of proliferation rates from 0.001 to 0.01 and 0.1 ng/mL of LIF in a lower cell density ($3.5x10^4$ cells/mL) was seen.

Cell density may influence the cell response to LIF, and a lower cell density can be important to conduct reliable proliferation assays. The proliferation assays in C2C12 and M1 cells are easy to perform and evaluate. Despite the results not corroborating all reports available in the literature, which may also be partially due to different sources of LIF used and cell origin (for example, primary mouse myoblasts and not C2C12 cell line), more assays are needed to validate the *in vitro* models. LIF is a pleiotropic cytokine and despite validation of this nanocarrier in these cell models, it has the potential to be applied in other areas such as, treatment of neurological diseases, infertility, lung protection after viral infections, among others.

7. Future perspectives

The optimal carrier is not achieved, and for that, it is necessary to reduce the protein concentration to improve the solubilization and consequently the encapsulation efficiency. For future application of this carriers *in vitro*, the hemolysis also revealed that they need to be used in low concentrations or functionalized with a stabilizing polymer like PEG to avoid toxicity and immune surveillance associated with cationic liposomes. This fact together with the release profile of the carrier need to be further optimized.

Because LIF triggers function when it is binds its receptor on the cell surface, it will also be important to produce another system, by ligating the protein to PEG on the exterior of the carrier, using PEG-maleimide. Both systems need to be compared in terms of size, surface charge, stability, and capacity to trigger cell response.

For future assays, it is necessary to confirm the parameters used in the *in vitro* models, possibly using a different commercial LIF.

8. Bibliography

[1] X. Yue, L. Wu, W. Hu, The Regulation of Leukemia Inhibitory Factor, Cancer Cell Microenviron. 2 (2015). https://doi.org/10.14800/ccm.877.

[2] N.A. Nicola, J.J. Babon, Leukemia inhibitory factor (LIF), Cytokine Growth Factor Rev. 26 (2015) 533–544. https://doi.org/10.1016/j.cytogfr.2015.07.001.

[3] J.-M. Cavaillon, M. Singer, T. Tanaka, M. Narazaki, T. Kishimoto, IL-6 Superfamily, Inflamm.: From Mol. Cell. Mech. to Clin. (2017) 573–586. https://doi.org/10.1002/9783527692156.ch23.

[4] NCBI, (2019). https://www.ncbi.nlm.nih.gov/gene/3976/ortholog/?scope=32523 (accessed January 3, 2019).

[5] M.G. Hinds, T. Maurer, J.G. Zhang, N.A. Nicola, R.S. Norton, Solution structure of leukemia inhibitory factor, J. Biol. Chem. 273 (1998) 13738–13745. https://doi.org/10.1074/jbc.273.22.13738.

[6] M.J. Boulanger, A.J. Bankovich, T. Kortemme, D. Baker, K.C. Garcia, Convergent mechanisms for recognition of divergent cytokines by the shared signaling receptor gp130, Mol. Cell. 12 (2003) 577–589. https://doi.org/10.1016/S1097-2765(03)00365-4.

[7] UniProt - Leukemia Inhibitory Factor, (2019). https://www.uniprot.org/uniprot/P09056 (accessed January 3, 2019).

[8] M. Mathieu, C. Saucourt, V. Mournetas, LIF-Dependent Signaling : New Pieces in the Lego, Stem Cell Rev. Reports. 1 (2012) 1–15. https://doi.org/10.1007/s12015-011-9261-7.

[9] R. Starr, U. Novak, T.A. Willson, M. Inglese, V. Murphy, W.S. Alexander, D. Metcalf, N.A. Nicola, D.J. Hilton, M. Ernst, Distinct roles for leukemia inhibitory factor receptor α-chain and gp130 in cell type-specific signal transduction, J. Biol. Chem. 272 (1997) 19982–19986. https://doi.org/10.1074/jbc.272.32.19982.

[10] C.M. Owczarek, Y. Zhang, M.J. Layton, D. Metcalf, B. Roberts, N.A. Nicola, The unusual species cross-reactivity of the leukemia inhibitory factor receptor α-chain is determined primarily by the immunoglobulin-like domain, J. Biol. Chem. 272 (1997) 23976–23985. https://doi.org/10.1074/jbc.272.38.23976.

[11] M.J. Layton, B.A. Cross, D. Metcalf, L.D. Ward, R.J. Simpson, N.A. Nicola, A major binding protein for leukemia inhibitory factor in normal mouse serum: Identification as a soluble form of the cellular receptor, Proc. Natl. Acad. Sci. U. S. A. 89 (1992) 8616–8620. https://doi.org/10.1073/pnas.89.18.8616.

[12] K. Imaizumi, S.I. Nishikawa, H. Tarui, T. Akuta, High-level expression and efficient one-step chromatographic purification of a soluble human leukemia inhibitory factor (LIF) in Escherichia coli, Protein Expr. Purif. 90 (2013) 20–26. https://doi.org/10.1016/j.pep.2013.04.006.

[13] G. Kaur, S.A. Ali, S. Pachauri, D. Malakar, J.K. Kaushik, A.K. Mohanty, S. Kumar, Buffalo Leukemia Inhibitory Factor Induces Differentiation and Dome-Like Secondary Structures in COS-1 Cells, Cytogenet. Genome Res. 151 (2017) 119–130. https://doi.org/10.1159/000465507.

[14] R. Kanegi, S. Hatoya, Y. Tsujimoto, S. Takenaka, T. Nishimura, V. Wijewardana, K. Sugiura, M. Takahashi, N. Kawate, H. Tamada, T. Inaba, Production of feline leukemia inhibitory factor with biological activity in Escherichia coli, Theriogenology. 86 (2015) 604–611. https://doi.org/10.1016/j.theriogenology.2016.02.013.

[15] S. Cui, L. Selwood, cDNA cloning, characterization, expression and recombinant protein production of leukemia inhibitory factor (LIF) from the marsupial, the brushtail possum (Trichosurus vulpecula), Gene. 243 (2000) 167–178. https://doi.org/10.1016/S0378-1119(99)00513-2.

[16] X. Xi, X. Li, F. Wu, X. Guan, L. Jin, Y. Guo, W. Song, B. Du, Expression, purification and characterization of active untagged recombinant human leukemia inhibitory factor from E coli, Protein Expr. Purif. (2017) 1–15. https://doi.org/10.1016/j.pep.2017.03.020.

[17] D.P. Gearing, N.A. Nicola, D. Metcalf, S. Foote, T.A. Willson, N.M. Gough, R.L. Williams, Production of leukemia inhibitory factor in escherichia coli by a novel procedure and iis use in maintaining embryonic stem cells in culture, Nat. Biotechnol. 7 (1989) 1157–1161. https://doi.org/10.1038/nbt1189-1157.

[18] H. Kang, Y. Park, Y. Lee, Y.J. Yoo, I. Hwang, Fusion of a highly N-glycosylated polypeptide increases the expression of ER-localized proteins in plants, Sci. Rep. 8 (2018) 1–10. https://doi.org/10.1038/s41598-018-22860-2.

[19] B.A. Youngblood, R. Alfano, S.C. Pettit, D. Zhang, H.G. Dallmann, N. Huang, C.C. MacDonald, Application of recombinant human leukemia inhibitory factor (LIF) produced in rice (Oryza sativa L.) for maintenance of mouse embryonic stem cells, J. Biotechnol. 172 (2014) 67–72. https://doi.org/10.1016/j.jbiotec.2013.12.012.

[20] D. Metcalf, D.P. Gearing, Fatal syndrome in mice engrafted with cells producing high levels of the leukemia inhibitory factor, Proc. Natl. Acad. Sci. U. S. A. 86 (1989) 5948–5952. https://doi.org/10.1073/pnas.86.15.5948.

[21] C.P. Santiago, C.J. Keuthan, S.L. Boye, S.E. Boye, A.A. Imam, J.D. Ash, A Drug-Tunable Gene Therapy for Broad-Spectrum Protection against Retinal Degeneration, Mol. Ther. 26 (2018) 2407–2417. https://doi.org/10.1016/j.ymthe.2018.07.016.

[22] B.B. Samal, T. Arakawa, T.C. Boone, T. Jones, S.J. Prestrelski, L.O. Narhi, J. Wen, G.W. Stearns, C.A. Crandall, J. Pope, S. Suggs, High level expression of human leukemia inhibitory factor (LIF) from a synthetic gene in Escherichia coli and the physical and biological characterization of the protein, Biochim. Biophys. Acta. 1260 (1995) 27–34.

[23] C. Jo, H. Kim, I. Jo, I. Choi, S. Jung, J. Kim, S. Soo, S. Ahn, Leukemia inhibitory factor blocks early differentiation of skeletal muscle cells by activating ERK, Elsevier. 1743 (2005) 187–197. https://doi.org/10.1016/j.bbamcr.2004.11.002.

[24] J.I. Aikawa, E.I. Sato, S. Kyuwa, E. Sato, K. Shiota, T. Ogawa, Asparagine-linked glycosylation of the rat leukemia inhibitory factor expressed by simian cos7 cells, Biosci. Biotechnol. Biochem. 62 (1998) 1318–1325. https://doi.org/10.1271/bbb.62.1318.

[25] C.H. Schmelzer, R.J. Harris, D. Butler, C.M. Yedinak, K.L. Wagner, L.E. Burton, Glycosylation Pattern and Disulfide Assignments of Recombinant Human Differentiation-Stimulating Factor, Arch. Biochem. Biophys. 302 (1993) 484–489. https://doi.org/10.1006/abbi.1993.1243.

[26] P. Goettig, Effects of glycosylation on the enzymatic activity and mechanisms of proteases, Int. J. Mol. Sci. 17 (2016) 1–24. https://doi.org/10.3390/ijms17121969.

[27] V. Pinho, M. Fernandes, A. da Costa, R. Machado, A.C. Gomes, Leukemia inhibitory factor: Recent advances and implications in biotechnology, Cytokine Growth Factor Rev. (2019) 1–9. https://doi.org/10.1016/j.cytogfr.2019.11.005.

[28] R.R. Seeley, Sistema muscular, in: Anat. e Fisiol., McGraw-Hill Higher Education, 2003: pp. 280–286.

[29] S.M. Abmayr, G.K. Pavlath, Myoblast fusion: lessons from flies and mice, Co. Biol. 139 (2012) 641–656. https://doi.org/10.1242/dev.068353.

[30] W. Yang, P. Hu, Skeletal muscle regeneration is modulated by inflammation, J. Orthop. Transl. 13 (2018) 25–32. https://doi.org/10.1016/j.jot.2018.01.002.

[31] C. Smith, M.J. Kruger, R.M. Smith, K.H. Myburgh, The Inflammatory Response to Skeletal Muscle Injury, Sport. Med. 38 (2008) 947–969. https://doi.org/10.2165/00007256-200838110-00005.

[32] L. Baoge, E. Van Den Steen, S. Rimbaut, N. Philips, E. Witvrouw, K.F. Almqvist, G. Vanderstraeten, L.C. Vanden Bossche, Treatment of Skeletal Muscle Injury: A Review, ISRN Orthop. (2012) 1–7. https://doi.org/10.5402/2012/689012.

[33] O. Thorsson, J. Rantanen, T. Hurme, H. Kalimo, Effects of nonsteroidal antiinflammatory medication on satellite cell proliferation during muscle regeneration., Am. J. Sports Med. 26 (1998) 172–6. http://www.ncbi.nlm.nih.gov/pubmed/9548108.

[34] T.L. Fernandes, A. Pedrinelli, A.J. Hernandez, Muscle injury: physiopathology, diagnostic, treatment and clinical presentation, Rev. Bras. Ortop. 46 (2011) 247–255. https://doi.org/10.1590/S0102-36162011000300003.

[35] L. Austin, A.W. Burgess, Stimulation of myoblast proliferation in culture by leukaemia inhibitory factor and other cytokines, J. Neurol. Sci. 101 (1991) 193–197. https://doi.org/10.1016/0022-510X(91)90045-9.

[36] D. Yaffe, O. Saxel, Serial passaging and differentiation of myogenic cells isolated from dystrophic mouse muscle, Nature. (1977) 725–727.

[37] P. Veliça, C.M. Bunce, A quick, simple and unbiased method to quantify C2C12 myogenic differentiation, Muscle and Nerve. 44 (2011) 366–370. https://doi.org/10.1002/mus.22056.

[38] N. Vakanis, J. Bower, L. Austin, In vitro myoblast to myotube transformations in the presence of leukemia inhibitory factor, Neurochem. Int. 27 (1995) 329–335.

[39] Y.-N. Jang, E.J. Baik, JAK-STAT pathway and myogenic differentiation, Jak-Stat. 2 (2013) e23282. https://doi.org/10.4161/jkst.23282.

[40] M. Pijet, B. Pijet, A. Litwiniuk, B. Pajak, B. Gajkowska, A. Orzechowski, Leptin impairs myogenesis in C2C12 cells through JAK/STAT and MEK signaling pathways, Cytokine. 61 (2013) 445–454. https://doi.org/10.1016/j.cyto.2012.11.002.

[41] M.J. Potthoff, E.N. Olson, MEF2: a central regulator of diverse developmental programs, Development. 134 (2007) 4131–4140. https://doi.org/10.1242/dev.008367.

[42] J.A.K. Stat, S. Pathway, Y. Diao, X. Wang, Z. Wu, SOCS1 , SOCS3 , and PIAS1 Promote Myogenic Differentiation by Inhibiting the Leukemia Inhibitory Factor-Induced, Cytokine. 29 (2009) 5084–5093. https://doi.org/10.1128/MCB.00267-09.

[43] Y. Yang, Y. Xu, W. Li, G. Wang, Y. Song, G. Yang, X. Han, Z. Du, L. Sun, K. Ma, STAT3 induces muscle stem cell differentiation by interaction with myoD, Cytokine. 46 (2009) 137–141. https://doi.org/10.1016/j.cyto.2008.12.015.

[44] F. Kasteng, P. Sobocki, C. Svedman, J. Lundkvist, Economic evaluations of leukemia: A review of the literature, Int. J. Technol. Assess. Health Care. 23 (2007) 43–53. https://doi.org/10.1017/S0266462307051562.

[45] M. Belson, B. Kingsley, A. Holmes, Risk factors for acute leukemia in children: A review, Environ. Health Perspect. 115 (2007) 138–145. https://doi.org/10.1289/ehp.9023.

[46] V.T. DeVita, E. Chu, A history of cancer chemotherapy, Cancer Res. 68 (2008) 8643–8653. https://doi.org/10.1158/0008-5472.CAN-07-6611.

[47] M. Sanz, A. Burnett, F. Lo-Coco, B. Lowenoerg, FLT3 inhibition as a targeted therapy for acute myeloid

leukemia, Curr. Opin. Oncol. 21 (2009) 594–600. https://doi.org/10.1097/CCO.0b013e32833118fd.

[48] M.W.N. Deininger, B.J. Druker, Specific targeted therapy of chronic myelogenous leukemia with imatinib, Pharmacol. Rev. 55 (2003) 401–423. https://doi.org/10.1124/pr.55.3.4.

[49] C.H. June, R.S. O'Connor, O.U. Kawalekar, S. Ghassemi, M.C. Milone, CAR T cell immunotherapy for human cancer, Science. 359 (2018) 1361–1365. https://doi.org/10.1126/science.aar6711.

[50] M. Kováč, M. Vášková, D. Petráčková, V. Pelková, E. Mejstříková, T. Kalina, M. Žaliová, J. Weiser, J. Starý, O. Hrušák, Cytokines, growth, and environment factors in bone marrow plasma of acute lymphoblastic leukemia pediatric patients, Eur. Cytokine Netw. 25 (2014) 8–13. https://doi.org/10.1684/ecn.2014.0348.

[51] T. Robak, A. Wierzbowska, M. Błasińska-Morawiec, A. Korycka, J.Z. Błoński, Serum levels of IL-6 type cytokines and soluble IL-6 receptors in active B-cell chronic lymphocytic leukemia and in cladribine induced remission, Mediators Inflamm. 8 (1999) 277–286. https://doi.org/10.1080/09629359990289.

[52] F. Zhou, R. Jin, Y. Hu, H. Mei, A novel BCR-ABL1 fusion gene with genetic heterogeneity indicates a good prognosis in a chronic myeloid leukemia case, Mol. Cytogenet. 10 (2017) 1–5. https://doi.org/10.1186/s13039-017-0322-8.

[53] W. Terpstra, B. Löwenberg, Application of myeloid growth factors in the treatment of acute myeloid leukemia, Leukemia. 11 (1997) 315–327. https://doi.org/10.1038/sj.leu.2400561.

[54] H.M. Mehta, M. Malandra, S.J. Corey, G-CSF and GM-CSF in Neutropenia, J. Immunol. 195 (2015) 1341–1349. https://doi.org/10.4049/jimmunol.1500861.

[55] T. Maekawa, D. Metcalf, D. P.Gearing, Enhanced supression of human myeloid leukemic cell lines by combination of IL-6, LIF, GM-CSF and G-CSF, Int. J. Cancer. 45 (1990) 353–358.

[56] M. Takanashi, T. Motoji, M.M. Masuda, K. Oshimi, H. Mizoguchi, THE EFFECTS OF LEUKEMIA INHIBITORY FACTOR AND INTERLEUKIN 6 ON THE GROWTH OF ACUTE MYELOID LEUKEMIA CELLS, Leuk. Res. 17 (1993) 217–222. https://doi.org/10.1017/CBO9781107415324.004.

[57] Acute myeloid leukemia and leukemia inhibitory factor - ClinicalTrials.Gov, (2019). https://clinicaltrials.gov/ct2/results?cond=Acute+Myeloid+Leukemia&term=%22Leukemia+inhibitory+factor%22&cntry=&state=&city=&dist= (accessed October 29, 2019).

[58] Acute myeloid leukemia and leukemia inhibitory factor - EU Clinical Trials Register, (2019). https://www.clinicaltrialsregister.eu/ctr-search/search?query=%22acute+myeloid+leukemia%22+AND+%22leukemia+inhbitory+factor%22 (accessed October 29, 2019).

[59] Y. Ichikawa, Differentiation of a cell line of myeloid leukemia, J. Cell. Physiol. 74 (1969) 223–234. https://doi.org/10.1002/jcp.1040740303.

[60] M. Minami, M. Inoue, S. Wei, K. Takeda, M. Matsumoto, T. Kishimoto, S. Akira, STAT3 activation is a critical step in gp130-mediated terminal differentiation and growth arrest of a myeloid cell line, Proc. Natl. Acad. Sci. U. S. A. 93 (1996) 3963–3966. https://doi.org/10.1073/pnas.93.9.3963.

[61] K.A. Lord, A. Abdollahi, S.M. Thomas, M. DeMarco, J.S. Brugge, B. Hoffman-Liebermann, D.A. Liebermann, Leukemia inhibitory factor and interleukin-6 trigger the same immediate early response, including tyrosine phosphorylation, upon induction of myeloid leukemia differentiation., Mol. Cell. Biol. 11 (1991) 4371–4379. https://doi.org/10.1128/mcb.11.9.4371.

[62] M. Selvakumaran, D.A. Liebermann, B. Hoffman-Liebermann, Deregulated c-myb disrupts interleukin-6- or

leukemia inhibitory factor-induced myeloid differentiation prior to c-myc: role in leukemogenesis., Mol. Cell. Biol. 12 (1992) 2493–2500. https://doi.org/10.1128/mcb.12.6.2493.

[63] T. Tanigawa, N. Nicola, G.A. McArthur, A. Strasser, C.G. Begley, Differential regulation of macrophage differentiation in response to leukemia inhibitory factor/oncostatin-M/interleukin-6: The effect of enforced expression of the SCL transcription factor, Blood. 85 (1995) 379–390.

[64] L.C. Moscinski, G. Kasnic, A. Saker, The significance of an elevated serum lysozyme value in acute myelogenous leukemia with eosinophilia, Am. J. Clin. Pathol. 97 (1992) 195–201. https://doi.org/10.1093/ajcp/97.2.195.

[65] M. Graf, S. Reif, T. Kroll, K. Hecht, V. Nuesler, H. Schmetzer, Expression of MAC-1 (CD11b) in Acute Myeloid Leukemia (AML) is associated with unfavorable prognosis, Am. J. Hematol. 81 (2006) 227–235. https://doi.org/10.1002/ajh.

[66] Y. Li, B. Chen, Induction of macrophage colony-stimulating factor receptor up-regulation in THP-1 human leukemia cells is dependent on the activation of C-FYN protein tyrosine kinase, Leuk. Res. 21 (1997) 539–547. https://doi.org/10.1016/S0145-2126(97)00004-0.

[67] J.A. Hamilton, G. Whitty, P. Masendycz, N.J. Wilson, J. Jackson, D. De Nardo, G.M. Scholz, The critical role of the colony-stimulating factor-1 receptor in the differentiation of myeloblastic leukemia cells, Mol. Cancer Res. 6 (2008) 458–467. https://doi.org/10.1158/1541-7786.MCR-07-0361.

[68] R.P. Feynman, There ' s Plenty of Room at the Bottom, J. Microeleciromechanical Syst. 1 (1992) 60–66. https://doi.org/10.1109/84.128057.

[69] K.E. Drexler, Nanotechnology: From Feynman to Funding, Bull. Sci. Technol. Soc. 24 (2004) 21–27. https://doi.org/10.1177/0270467604263113.

[70] N. Science, T. Council, National Nanotechnology Initiative - Leading To the Next Industrial Revolution, Microscale Thermophys. Eng. 4 (2000) 205–212. https://doi.org/10.1080/10893950050148160.

[71] R.E. Smalley, Of chemistry, love and nanobots., Sci. Am. 285 (2001) 76–77. https://doi.org/10.1038/scientificamerican0901-76.

[72] B.G. Sheeparamatti, Nanotechnology : Inspiration from Nature, IETE Techinal Rev. 24 (2007) 5–8.

[73] A. Selim, A. Lila, T. Ishida, Liposomal Delivery Systems : Design Optimization and Current Applications, Pharm. Soc. Japan. 40 (2017) 1–10.

[74] A.C.N. Oliveira, J. Fernandes, A. Gonçalves, A.C. Gomes, M.E.C.D.R. Oliveira, Lipid-based Nanocarriers for siRNA Delivery: Challenges, Strategies and the Lessons Learned from the DODAX: MO Liposomal System, Curr. Drug Targets. 20 (2018) 29–50. https://doi.org/10.2174/1389450119666180703145410.

[75] T.B. Soares, L. Loureiro, A. Carvalho, M.E.C.D.R. Oliveira, A. Dias, B. Sarmento, M. Lúcio, Lipid nanocarriers loaded with natural compounds: Potential new therapies for age related neurodegenerative diseases?, Prog. Neurobiol. 168 (2018) 21–41. https://doi.org/10.1016/j.pneurobio.2018.04.004.

[76] S.J. Soenen, P. Rivera-Gil, J.M. Montenegro, W.J. Parak, S.C. De Smedt, K. Braeckmans, Cellular toxicity of inorganic nanoparticles: Common aspects and guidelines for improved nanotoxicity evaluation, Nano Today. 6 (2011) 446–465. https://doi.org/10.1016/j.nantod.2011.08.001.

[77] R. Nisini, N. Poerio, S. Mariotti, F. De Santis, M. Fraziano, The multirole of liposomes in therapy and prevention of infectious diseases, Front. Immunol. 9 (2018). https://doi.org/10.3389/fimmu.2018.00155.

[78] A. Akbarzadeh, R. Rezaei-Sadabady, S. Davaran, S.W. Joo, N. Zarghami, Y. Hanifehpour, M. Samiei, M. Kouhi, K. Nejati-Koshki, Liposome: Classification, preparation, and applications, Nanoscale Res. Lett. 8 (2013) 1–8. https://doi.org/10.1186/1556-276X-8-102.

[79] M. Fernandes, I. Lopes, J. Teixeira, C. Botelho, A.C. Gomes, Exosome-Like Nanoparticles: A New Type Of Nanocarrier, Curr. Med. Chem. 26 (2019) 1–15. https://doi.org/10.2174/0929867326666190129142604.

[80] C. Tanford, The Hydrophobic Effect and the Organization of Living Matter Charles Tanford, AAAS. 200 (1978) 1012–1018.

[81] P. V. Escribá, Membrane-lipid therapy: A new approach in molecular medicine, Trends Mol. Med. 12 (2006) 34–43. https://doi.org/10.1016/j.molmed.2005.11.004.

[82] J. Li, X. Wang, T. Zhang, C. Wang, Z. Huang, X. Luo, Y. Deng, A review on phospholipids and their main applications in drug delivery systems, Asian J. Pharm. Sci. 10 (2015) 81–98. https://doi.org/10.1016/j.ajps.2014.09.004.

[83] D.M. Owen, Methods in membrane lipids: Second edition, Methods Membr. Lipids Second Ed. 1232 (2014) 307–322. https://doi.org/10.1007/978-1-4939-1752-5.

[84] K. Bacia, J. Schweizer, Practical Course : Giant Unilamellar Vesicles, (2005) 1–18.

[85] F. Gambinossi, S.E. Mylon, J.K. Ferri, Aggregation kinetics and colloidal stability of functionalized nanoparticles, Adv. Colloid Interface Sci. 222 (2015) 332–349. https://doi.org/10.1016/j.cis.2014.07.015.

[86] I. Lopes, A. C. N. Oliveira, M. P. Sárria, J. P. Neves Silva, O. Gonçalves, A.C. Gomes, M.E.C.D. Real Oliveira, Monoolein-based nanocarriers for enhanced folate receptor-mediated RNA delivery to cancer cells, J. Liposome Res. 26 (2016) 199–210. https://doi.org/10.3109/08982104.2015.1076463.

[87] C. Carneiro, A. Correia, T. Collins, M. Vilanova, C. Pais, A.C. Gomes, M.E.C.D. Real Oliveira, P. Sampaio, DODAB:monoolein liposomes containing Candida albicans cell wall surface proteins: A novel adjuvant and delivery system, Eur. J. Pharm. Biopharm. 89 (2015) 190–200. https://doi.org/10.1016/j.ejpb.2014.11.028.

[88] A.C.N. Oliveira, T.F. Martens, K. Raemdonck, R.D. Adati, E. Feitosa, C. Botelho, A.C. Gomes, K. Braeckmans, M.E.C.D. Real Oliveira, Dioctadecyldimethylammonium:monoolein nanocarriers for efficient in vitro gene silencing, ACS Appl. Mater. Interfaces. 6 (2014) 6977–6989. https://doi.org/10.1021/am500793y.

[89] A.C.N. Oliveira, K. Raemdonck, T. Martens, K. Rombouts, R. Simón-Vázquez, C. Botelho, I. Lopes, M. Lúcio, Á. González-Fernández, M.E.C.D. Real Oliveira, A.C. Gomes, K. Braeckmans, Stealth monoolein-based nanocarriers for delivery of siRNA to cancer cells, Acta Biomater. 25 (2015) 216–229. https://doi.org/10.1016/j.actbio.2015.07.032.

[90] J.P.N. Silva, I.M.S.C. Oliveira, A.C.N. Oliveira, M. Lúcio, A.C. Gomes, P.J.G. Coutinho, M.E.C.D.R. Oliveira, Structural dynamics and physicochemical properties of pDNA/DODAB:MO lipoplexes: Effect of pH and anionic lipids in inverted non-lamellar phases versus lamellar phases, Biochim. Biophys. Acta - Biomembr. 1838 (2014) 2555–2567. https://doi.org/10.1016/j.bbamem.2014.06.014.

[91] J.P.N. Silva, A.C.N. Oliveira, M.P.P.A. Casal, A.C. Gomes, P.J.G. Coutinho, O.P. Coutinho, M.E.C.D.R. Oliveira, DODAB:monoolein-based lipoplexes as non-viral vectors for transfection of mammalian cells, Biochim. Biophys. Acta - Biomembr. 1808 (2011) 2440–2449. https://doi.org/10.1016/j.bbamem.2011.07.002.

[92] J.P.N. Silva, A.C.N. Oliveira, M. Lúcio, A.C. Gomes, P.J.G. Coutinho, M.E.C.D.R. Oliveira, Tunable pDNA/DODAB: MO lipoplexes: The effect of incubation temperature on pDNA/DODAB: MO lipoplexes structure and transfection efficiency, Colloids Surfaces B Biointerfaces. 121 (2014) 371–379. https://doi.org/10.1016/j.colsurfb.2014.06.019.

[93] C. Carneiro, A. Correia, T. Lima, M. Vilanova, C. Pais, A.C. Gomes, M.E.C.D. Real Oliveira, P. Sampaio, Protective effect of antigen delivery using monoolein-based liposomes in experimental hematogenously disseminated candidiasis, Acta Biomater. 39 (2016) 133–145. https://doi.org/10.1016/j.actbio.2016.05.001.

[94] A.C.N. Oliveira, S.S. Nogueira, O. Gonçalves, M.F. Cerqueira, P. Alpuim, J. Tovar, C. Rodriguez-Abreu, G. Brezesinski, A.C. Gomes, M. Lúcio, M.E.C.D.R. Oliveira, Role of counter-ion and: Helper lipid content in the design and properties of nanocarrier systems: A biophysical study in 2D and 3D lipid assemblies, RSC Adv. 6 (2016) 47730–47740. https://doi.org/10.1039/c6ra08125h.

[95] I.M.S.C. Oliveira, J.P.N. Silva, E. Feitosa, E.F. Marques, E.M.S. Castanheira, M.E.C.D. Real Oliveira, Aggregation behavior of aqueous dioctadecyldimethylammonium bromide/monoolein mixtures: A multitechnique investigation on the influence of composition and temperature, J. Colloid Interface Sci. 374 (2012) 206–217. https://doi.org/10.1016/j.jcis.2012.01.053.

[96] P. Taylor, G. Dékány, I. Csóka, I. Erös, Interaction Between Liposomes and Neutral Polymers : Effect of Adsorption on Drug Release Interaction Between Liposomes and Neutral Polymers : Effect of Adsorption on Drug Release, J. Dispers. Sci. Technol. 22 (2007) 37–41.

[97] L.K. Müller, K. Landfester, Natural liposomes and synthetic polymeric structures for biomedical applications, Biochem. Biophys. Res. Commun. 468 (2015) 411–418. https://doi.org/10.1016/j.bbrc.2015.08.088.

[98] B. Romberg, W.E. Hennink, G. Storm, Sheddable coatings for long-circulating nanoparticles, Pharm. Res. 25 (2008) 55–71. https://doi.org/10.1007/s11095-007-9348-7.

[99] Bio-rad, Protein assays: Colorimetric Protein Assays, 1975. www.bio-rad.com/webroot/web/pdf/lsr/literature/Bulletin_1069.pdf.

[100] N.J. Kruger, The Bradford Method for Protein Quantification, (2009) 17–24.

[101] I.E.A. Lopes, Development of stable lipoplexes DODAC- MO - PEG-FOL for delivery of nucleic acids to cells expressing folate receptor, 2013. http://repositorium.sdum.uminho.pt/handle/1822/25568.

[102] E.A. Orellana, A.L. Kasinski, Sulforhodamine B (SRB) Assay in Cell Culture to Investigate Cell Proliferation, Bio-Protocol. 6 (2017) 1–9. https://doi.org/10.21769/BioProtoc.1984.Sulforhodamine.

[103] A.J.A.M. Ribeiro, A.C. Gomes, A.M. Cavaco-paulo, Developing scaffolds for tissue engineering using the Ca 2 þ -induced cold gelation by an experimental design approach, Soc. Biomater. (2012) 2269–2278. https://doi.org/10.1002/jbm.b.32797.

[104] W. Strober, Trypan Blue Exclusion Test of Cell Viability, Curr. Protoc. Immunol. 111 (2015) 1–3. https://doi.org/10.1002/0471142735.ima03bs111.

[105] A.C.N. Oliveira, M.P. Sária, P. Moreira, J. Fernandes, L. Castro, I. Lopes, M. Côrte-Real, A. Cavaco-Paulo, M.E.C.D. Real Oliveira, A.C. Gomes, Counter ions and constituents combination affect DODAX:MO nanocarriers toxicity: In vitro and in vivo, Toxicol. Res. 5 (2016) 1244–1255. https://doi.org/10.1039/c6tx00074f.

[106] E.Y. Chi, S. Krishnan, T.W. Randolph, J.F. Carpenter, Physical stability of proteins in aqueous solution: Mechanism and driving forces in nonnative protein aggregation, Pharm. Res. 20 (2003) 1325–1336.

https://doi.org/10.1023/A:1025771421906.

9. Supplementary data

PBS 10x: Weight 22.7g of Na2HPO4, 2.4 g of KH2PO4, 80g of NaCl and 2g of KCL. Add to 800mL of ultrapure water and adjust the pH to 7.3. Add water until the final volume is 1L.

Table S1 Results from stability for 0.2mM DODAB:MO empty in pH 5 at 37°C.

Timepoints	Population 1 (nm)	Intensity (%)	Population 2	Intensity	Population 3	% Intensity
0h	196.2	91,6	32.48	8.4	0	0
30 min	223.5	92,2	36.49	7.8	0	0
1h	352.5	95,4	30.6	4.6	0	0
2h	214.9	100	0	0	0	0
3h	238.1	92,7	42.57	7.3	0	0
4h	237.7	95,4	34.15	4.6	0	0
5h	248.9	97	23.85	3	0	0
6h	257.8	91,2	44.44	8.8	0	0

Table S2 Results from stability for 0.2mM DODAB:MO empty in pH 7.4 at 37°C.

Timepoints	Population 1 (nm)	Intensity (%)	Population 2	Intensity	Population 3	% Intensity
0h	337.5	93.2	53.11	5.7	0	0
30 min	383.1	98.6	5132	1.4	0	0
1h	387.9	100	0	0	0	0
2h	366.6	100	0	0	0	0
3h	457.2	97.1	4649	2.9	0	0
4h	494.7	100	0	0	0	0
5h	307	100	0	0	0	0
6h	297.2	100	0	0	0	0

Table S3 Results from stability for 0.2mM DODAB:MO empty in 25% FBS at 37°C.

Timepoints	Population 1 (nm)	Intensity (%)	Population 2	Intensity	Population 3	% Intensity
0h	453.5	81.9	34.73	10.6	8.12	7.5
30 min	360	76.2	40.68	11.6	9.267	8.5
1h	332.3	77.2	37.06	14.6	8.109	8.2
2h	555.9	80.7	35.41	9.9	8.405	6.3
3h	332.7	76.7	42,32	14	8,971	9,3
4h	323	77,4	48.18	11.8	10.33	10.8
5h	314.7	78.9	40.73	11.7	9.015	9.4
6h	307.7	80.5	32.43	12	7.851	7.5

Table S4 Results from stability for 0.2mM DODAB:MO encapsulating 5 ug/mL of BSA in pH 5 at 37°C.

Timepoints	Population 1 (nm)	Intensity (%)	Population 2	Intensity	Population 3	% Intensity
0h	225	94.9	29.2	5.1	0	0
30 min	224.1	100	0	0	0	0
1h	232.1	100	0	0	0	0
2h	245.7	100	0	0	0	0
3h	275.3	100	0	0	0	0
4h	252.7	100	0	0	0	0
5h	252.4	100	0	0	0	0
6h	276.4	100	0	0	0	0

Table S5 Results from stability for 0.2mM DODAB:MO encapsulating 5 ug/mL of BSA in pH 7.4 at 37°C.

Timepoints	Population 1 (nm)	Intensity (%)	Population 2	Intensity	Population 3	% Intensity
0h	367.2	95.8	52.97	4.2	0	0
30 min	394.7	96	67.72	4	0	0
1h	396.6	100	0	0	0	0
2h	627.3	78.5	159.1	19.3	0	0
3h	487.8	95.9	4761	4.1	0	0
4h	449.8	90.9	4535	7.6	0	0
5h	465.4	95.8	4982	4.2	0	0
6h	361.2	95.2	4316	4.8	0	0

Table S6 Results from stability for 0.2mM DODAB:MO encapsulating 5 ug/mL of BSA in 25% at 37°C.

Timepoints	Population 1 (nm)	Intensity (%)	Population 2	Intensity	Population 3	% Intensity
0h	334.2	78.5	36.73	12.9	7.980	8.6
30 min	340.7	73.7	43.52	16.3	8.353	10.1
1h	430.7	73.4	38.63	12.7	7.951	7.7
2h	475.4	77.1	45.08	12.6	8.770	7.8
3h	587.7	81.2	46.25	12.5	8.046	6.3
4h	1177	87.6	26.68	7.4	9.214	5.0
5h	322.4	73.2	42.14	15.9	8.598	10.9
6h	314.6	74.8	37.95	14.5	8.954	10.6

Table S7 Results from stability for 0.2mM DODAB:MO encapsulating 10 ug/mL of BSA in pH 7.4 at 37°C

Timepoints	Population 1 (nm)	Intensity (%)	Population 2	Intensity	Population 3	% Intensity
0h	233.5	93.2	32.91	6.8	0	0
30 min	199.4	98.3	12.33	1.7	0	0
1h	191.2	100	0	0	0	0
2h	199.1	97.6	24.35	1.6	0	0
3h	198.1	100	0	0	0	0
4h	219.4	100	0	0	0	0
5h	207.9	93.6	37.07	6.4	0	0
6h	207	100	0	0	0	0

Table S8 Results from stability for 0.2mM DODAB:MO encapsulating 10 ug/mL of BSA in pH 7.4 at 37°C.

Timepoints	Population 1 (nm)	Intensity (%)	Population 2	Intensity	Population 3	% Intensity
0h	212.4	96.9	27.54	3.1	0	0
30 min	252.5	100	0	0	0	0
1h	220.5	98.5	4978	1.5	0	0
2h	235.5	100	0	0	0	0
3h	255.8	97.9	4405	2.1	0	0
4h	382.3	99.9	4916	0.1	0	0
5h	221.2	96.9	4530	3.1	0	0
6h	248.7	100	0	3.1	0	0

Table S9 Results from stability for 0.2mM DODAB:MO encapsulating 10 ug/mL of BSA in 25% FBS at 37°C.

Timepoints	Population 1 (nm)	Intensity (%)	Population 2	Intensity	Population 3	% Intensity
0h	481.1	67.7	45.32	19.5	8.797	12.8
30 min	528.1	70.9	33.87	18.1	7.023	11.0
1h	429.2	66.4	40.14	20.4	8.531	13.2
2h	864.5	74.8	33.14	15.08	7.923	9.5
3h	295.9	73.0	10.07	14.8	35.31	10.7
4h	535.5	63.8	12.98	18.9	68.19	17.3
5h	416.0	65.0	42.03	19.6	9.519	15.4
6h	N.D	N.D	N.D	N.D	N.D	N.D

Table S10 Results from stability for 0.2mM DODAB:MO encapsulating 5 µg/mL of LIF in pH 5 at 37°C.

Timepoints	Population 1 (nm)	Intensity (%)	Population 2	Intensity	Population 3	% Intensity
0h	221.1	91.1	43.25	9.0	0	0
30 min	213.7	91.9	42.97	8.1	0	0
1h	234.0	93.0	20.62	3.0	0	0
2h	207.5	100	0	0	0	0
3h	253.8	100	0	0	0	0
4h	236.0	97.5	3825	2.5	0	0
5h	233.4	98.3	4366	1.7	0	0
6h	266.2	97.2	5025	2.8	0	0

Table S11 Results from stability for 0.2mM DODAB:MO encapsulating 5 µg/mL of LIF in pH 7.4 at 37°C.

Timepoints	Population 1 (nm)	Intensity (%)	Population 2	Intensity	Population 3	% Intensity
0h	5062	84.6	84.69	15.4	0	0
30 min	210.2	98.7	5072	1.3	0	0
1h	255.8	94.8	4194	5.2	0	0
2h	213.1	100	0	0	0	0
3h	220	100	0	0	0	0
4h	199.5	96.7	4853	3.3	0	0
5h	212.8	90.2	1970	9.8	0	0
6h	195.6	96.5	4527	3.5	0	0

Table S12 Results from stability for 0.2mM DODAB:MO encapsulating 5 µg/mL of LIF in 25% FBS at 37°C.

Timepoints	Population 1 (nm)	Intensity (%)	Population 2	Intensity	Population 3	% Intensity
0h	996.8	62.3	206.9	37.7	0	0
30 min	774.7	100	0	0	0	0
1h	676.8	92.1	30.77	3.8	9,28	2.7
2h	646.0	90.7	77.64	5.6	12.21	3.7
3h	375.9	94.0	42.62	6.0	0	0
4h	370.9	98.2	4670	1.8	0	0
5h	556.8	94.5	8.346	3.3	24.72	2.2
6h	498.0	96.7	4963	3.3	0	0